Earth and Space Science

RESEARCH ARTICLE
10.1029/2019EA000679

# Export Flux, Biogeochemical Effects, and the Fate of a Terrestrial Carbonate System: From Changjiang (Yangtze River) Estuary to the East China Sea

**Tian-qi Xiong[1], Peng-fei Liu[2], Wei-dong Zhai[1,3], Yan Bai[4], Dong Liu[5], Di Qi[6], Nan Zheng[7], Jin-wen Liu[6], Xiang-hui Guo[3], Tian-yu Cheng[8], Hai-xia Zhang[1], Song-yin Wang[1], Xian-qiang He[4], Jian-fang Chen[4], and Ru Li[7]**

[1]Institute of Marine Science and Technology, Shandong University, Qingdao, China, [2]State Key Laboratory of Marine Geology, Tongji University, Shanghai, China, [3]State Key Laboratory of Marine Environmental Science, Xiamen University, Xiamen, China, [4]State Key Laboratory of Satellite Ocean Environment Dynamics, Second Institute of Oceanography, Ministry of Natural Resources, Hangzhou, China, [5]Key Laboratory of Watershed Geographic Sciences, Nanjing Institute of Geography and Limnology, Chinese Academy of Sciences, Nanjing, China, [6]Key Laboratory of Global Change and Marine-Atmospheric Chemistry of Ministry of Natural Resources, Third Institute of Oceanography, Ministry of Natural Resources, Xiamen, China, [7]National Marine Environmental Monitoring Center, Dalian, China, [8]Shanghai Marine Environmental Monitoring and Forecasting Center, Shanghai, China

**Key Points:**
- Changjiang (Yangtze River) export flux of total alkalinity varied around a nearly stable average over the past 55 years
- Terrestrial carbonate input from Changjiang decreased the freshwater-dilution-induced coastal aragonite saturation state suppression by 12%
- More than 10% of wet-season DIC flux discharged from Changjiang was sequestered in coastal zones, while the TAlk flux was rarely affected

**Supporting Information:**
- Supporting Information S1

**Correspondence to:**
W.-d. Zhai,
wdzhai@126.com
wdzhai@sdu.edu.cn

**Citation:**
Xiong, T.-q., Liu, P.-f., Zhai, W.-d., Bai, Y., Liu, D., Qi, D., et al. (2019). Export flux, biogeochemical effects, and the fate of a terrestrial carbonate system: From Changjiang (Yangtze River) Estuary to the East China Sea. *Earth and Space Science*, *6*, 2115–2141. https://doi.org/10.1029/2019EA000679

Received 18 APR 2019
Accepted 11 OCT 2019
Accepted article online 8 NOV 2019
Published online 21 NOV 2019

Tian-qi Xiong and Peng-fei Liu Equal contribution.



**Abstract** Seasonal variations in the transports of total alkalinity (TAlk) and dissolved inorganic carbon (DIC) from the Lower Changjiang (Yangtze) River/Estuary to the East China Sea were investigated based on a series of field surveys in 2015–2017, including monthly samplings at Datong Station and seasonal mapping cruises in the Changjiang Estuary and the adjacent northwestern East China Sea. In comparison with historical data sets, the Changjiang TAlk flux varied around a nearly stable average over the past 55 years. This is much different from some American rivers, where TAlk export fluxes increased for a century long. To assess effects of riverine carbonate inputs on coastal carbonate chemistry, we compared several cases showing freshwater-dilution-induced decline in coastal aragonite saturation state ($\Omega_{arag}$), including rainwater dilution and riverine water dilution. Without riverine carbonate inputs, the effect of a unit of salinity decrease (due to rainwater dilution) on $\Omega_{arag}$ was expected to be counteracted by a DIC removal of 10 μmol/kg relative to the baseline value along relevant conservative mixing line, when coastal $\Omega_{arag}$ was close to a critical value of 1.5. Considering terrestrial carbonate inputs from Changjiang, however, the freshwater-dilution-induced coastal $\Omega_{arag}$ suppression decreased by 12%. Our data also showed that more than 10% of wet-season DIC flux discharged from the Changjiang Estuary was sequestered by biological activities in nearshore areas, while the TAlk flux was rarely affected. This biological alteration effectively transformed the terrestrial carbonate system from a feature of DIC:TAlk >1.0 to the usual seawater feature of DIC:TAlk <0.9.

**Plain Language Summary** Changjiang (Yangtze River) serves as the second largest carbonate contributor to the ocean among the world large rivers. We examined riverine/estuarine transport fluxes of total alkalinity (TAlk) and dissolved inorganic carbon (DIC) in the continuum from the Lower Changjiang to its estuary and to the adjacent northwestern East China Sea. In comparison with historical data, the Changjiang TAlk flux varied around a nearly stable average over the past 55 years, which was much different from the American case of century-long TAlk increase in some rivers. We also assessed effects of riverine carbonate inputs on the coastal carbonate chemistry. Results suggest that terrestrial carbonate inputs decreased the freshwater-dilution-induced carbonate mineral suppression in coastal zones. Based on field data, we estimated that more than 10% of wet-season DIC flux discharged from the Changjiang Estuary was sequestered by biological activities in nearshore areas, while the TAlk flux was rarely affected. We explained how biological drawdown of riverine DIC transformed the terrestrial feature of DIC:TAlk ratio higher than 1.0 to the usual seawater feature of DIC:TAlk ratio less than 0.9, supporting Alfred C. Redfield's argument on "the influence of organisms on the composition of seawater" in the 1960s or earlier.

## 1. Introduction

Rivers and estuaries connect terrestrial and oceanic carbon reservoirs, discharging a dissolved inorganic carbon (DIC) flux of $0.4\times10^{15}$ g/year to the ocean (Bauer et al., 2013; Meybeck, 1993; Prentice et al., 2001). In

many temperate and subtropical rivers, such as the American Mississippi (Dagg et al., 2005; Guo et al., 2012), Delaware River (Joesoef et al., 2017), European Tagus River (Oliveira et al., 2017), and Asian Pearl River, China (Guo et al., 2008), the DIC is mostly composed of $HCO_3^-$ ion, which is the major chemical production of carbonate and silicate weathering. The $HCO_3^-$ ion concentration also dominates total alkalinity (TAlk). The latter is defined as the sum of $[HCO_3^-]$, $2[CO_3^{2-}]$, $[B(OH)_4^-]$, $[OH^-]$ and all other weak bases in water that can accept $H^+$ ions when titrated to the carbonic acid endpoint (Dickson, 1992). These DIC and TAlk fluxes affect coastal carbonate dynamics, with particularly acute influences on carbonate saturation states ($\Omega$, which is defined as $[Ca^{2+}] \times [CO_3^{2-}] / K_{sp}^*$, where $K_{sp}^*$ is the apparent solubility product for either calcite or aragonite, the two major mineral forms of $CaCO_3$) that is necessary for growths of shellfishes and many other calcifiers (Hu et al., 2017; Jiang et al., 2010; Salisbury et al., 2008).

To measure terrestrial inorganic carbon or TAlk in the ocean, DIC or TAlk values are usually assumed to be linearly related to salinity, i.e. considering water dilution only (Friis et al., 2003; Fry et al., 2015; Zhai, Chen, et al., 2014). However, precipitation and evaporation in open oceans also affect DIC and TAlk in proportion with salinity. This makes it difficult to differentiate the terrestrial DIC and TAlk in a coastal setting from the salinity-based mixing with marine sources. Therefore, neither salinity normalized DIC nor salinity normalized TAlk is a qualified single parameter for identifying terrestrial signals from seawater DIC and TAlk values.

Open oceans typically have DIC:TAlk ratios of <0.9 (e.g., Takahashi et al., 2014; Wang, Wanninkhof, et al., 2013; Zhai & Zhao, 2016), strikingly different from the riverine carbonate system. The latter is usually characterized by a DIC:TAlk ratio of slightly higher than or nearly equal to 1. Even in tropical rivers such as the Amazon and Congo Rivers, DIC:TAlk ratios are as high as 1.5–3, since these river waters contain high concentrations of free $CO_2$ (Aufdenkampe et al., 2011; Körtzinger, 2003; Wang, Bienvenu, et al., 2013). We contend that the DIC:TAlk ratio is a better geochemical indicator than the salinity normalized TAlk (also better than the salinity normalized DIC) to distinguish between terrestrial carbonate system and oceanic carbonate system. So far, it remains unclear how the terrestrial carbonate system is transformed into the seawater carbonate system in coastal oceans. To better understand the fate of riverine DIC in estuaries and coastal zones, more regional studies are needed, especially in large-river estuaries such as the Changjiang Estuary.

In addition, recent evidence suggests that humans have altered inorganic carbon fluxes in some river-estuary continuums (e.g., Cai et al., 2008; Raymond & Cole, 2003; Regnier et al., 2013). The Mississippi and some other American rivers increased their bicarbonate ($HCO_3^-$) export fluxes by ~70% in the twentieth century, mainly owing to mining and land use changes causing an anthropogenic enhancement of chemical weathering (Kaushal et al., 2013; Raymond et al., 2008). In the Mississippi basin, for example, ~20 g $CaCO_3 \cdot m^{-2}$ cropland $\cdot$ $year^{-1}$ was introduced to neutralize acidic soil (Oh & Raymond, 2006; West & McBride, 2005). This large-scale agricultural practice of liming undoubtedly increases the riverine transport flux of TAlk. However, Asian rivers behave differently from the American rivers. For example, the lower Yellow River showed simultaneous declines in water discharge and material fluxes in the past 50 years (Wang, Yang, et al., 2006; Wang et al., 2010). In Changjiang (Yangtze River), the Three Gorges Dam started its first filling stage during June 2003 to May 2006 at ~2,000 km upstream from the river mouth of Changjiang. Although the decline in transport flux of suspended particle matters in Changjiang has been well documented in literatures (e.g., Dai et al., 2011; Zhao et al., 2015), the possible disturbance of the Three Gorges Dam to Changjiang DIC discharge is still unstudied.

Moreover, the ocean acidification problem in response to increasing atmospheric $CO_2$ (Caldeira & Wickett, 2003; Doney et al., 2009; Orr et al., 2005) strikes at biotopes of many coastal oceans. Owing to the combined effect of the atmospheric $CO_2$ invasion and some local oceanographic processes, the coastal acidification will likely worsen in the coming decades (e.g., Cai et al., 2011; Ekstrom et al., 2015; Li & Zhai, 2019). For example, low aragonite saturation state index ($\Omega_{arag}$) was frequently observed in coastal zones due to freshwater inputs (Hu et al., 2017; Jiang et al., 2010; Salisbury et al., 2008; Zhai et al., 2015). Although Chou et al. (2013) have investigated the freshwater dilution effect on $\Omega_{arag}$ dynamics in relatively high-salinity areas in the Changjiang Estuary, such effects in large estuaries with huge amounts of freshwater and riverine inorganic carbon inputs are still poorly understood.

Chemically, $\Omega_{arag} > 1$ indicates that the $CaCO_3$ mineral of aragonite is stable in the seawater, while $\Omega_{arag} < 1$ indicates that the mineral is unstable. Based on a field data investigation, Li and Zhai (2019) revealed that

the summertime net community calcification rate in subsurface waters of the North Yellow Sea declined to zero when the $\Omega_{arag}$ value reached the critical level of 1.5–1.6. In this study, to determine the severity of the threat of low-$\Omega_{arag}$ seawater in coastal oceans to marine calcifying organisms, we used an $\Omega_{arag}$ value of 1.5 as a critical threshold for marine shellfish development (e.g., Ekstrom et al., 2015; Gruber et al., 2012; Waldbusser et al., 2015).

In this study, we examined riverine/estuarine transport fluxes of TAlk and DIC in the continuum from Lower Changjiang to its estuary and to the adjacent northwestern East China Sea (ECS; Figure 1a). By comparing our time-series data obtained during 2005–2017 with historical data over the past 5 decades, long-term variations of TAlk and DIC fluxes were studied. Using new field data obtained from our seasonal mapping cruises carried out in the Changjiang Estuary during 2015–2017, we studied potential effects of the Changjiang carbonate inputs on the coastal zone carbonate chemistry. Together with earlier-obtained datasets, we also attempted to better understand the fate of terrestrial inorganic carbon on the shelf. This understanding is essential for closing carbon budgets in river-dominated ocean margins of scientific importance.

## 2. Materials and Methods

### 2.1. Study Area

Changjiang (Yangtze River) is the world's 4th largest river by virtue of water discharge (Dai & Trenberth, 2002), accounting for 90–95% of the total riverine water inputs into the ECS (Chen et al., 2001). Its drainage area of $1.8\times10^6$ $km^2$ covers 20% of the total terrestrial area of China, where extensive agriculture has been sustained for thousands of years, nowadays nourishing 30% of the population of China (http://www.cjw.gov.cn/zjzx/cjyl/lyxz/). Changjiang originates in the Tibetan Plateau and flows eastward through the Yun-Gui Plateau, Sichuan Basin and the Three-Gorges region, where the basement rocks are abundant in carbonates (Chen et al., 2002). Then it drains the subtropical plains in central and eastern China and finally enters the ECS. Changjiang is characterized by rather high alkalinity and carbonate weathering rates as compared with many other major rivers in the world (Gaillardet et al., 1999).

Datong Station is the hydrological station located farthest downstream in Changjiang, 624 km upstream from the river mouth (Figure 1b), sampling 95% of the entire Changjiang watershed. The river course at the Station is 1,800 m wide and ~30 m deep at the highest water level (Figures 1c and 1d).

Approximately 330 km downstream from Datong Station, Chongming Island develops (Figure 1b) due to long-term estuarine sedimentary processes. The areas between 121°E (the west side of Chongming Island) and 122°E are regarded as the inner Changjiang Estuary (Zhai et al., 2007). The present-day inner Changjiang Estuary is about 120 km long and more than 90 km wide at its outlet, including two primary branches divided by Chongming Island. The South Branch connects to the ECS through three deep passages with a water depth of 20 m, while the North Branch features numerous intertidal zones with shallow water depths of 1 to 8 m (Zhai et al., 2017). From the South Branch to the ECS, a salinity front develops around 122°E, where surface-water salinity varied from <10 in the inner estuary to typically 10–31 in the outer estuary (Zhai et al., 2007). The Changjiang Estuary has several local sources of TAlk and DIC from Huangpujiang River, a downstream major tributary of Changjiang (Zhai et al., 2007), from the North Branch of Changjiang Estuary (Zhai et al., 2017), and from tidal marshes east to Chongming Island where anaerobic processes such as denitrification occur in sediment (Wang, Chen, et al., 2006). The influence of Changjiang river plume, that is, Changjiang Diluted Water (CDW) extends hundreds of kilometers offshore (Bai et al., 2014). The enormous freshwater discharge and nutrient and sediment loads greatly affect biogeochemical processes in the western ECS (Chen et al., 2008; Gong et al., 2000). For example, intensive algal blooms were usually observed in this region in spring and summer, mostly due to increasing nutrient inputs from the Changjiang River during the two seasons (e.g., Chen et al., 2003; He et al., 2013; Zhai, Chen, et al., 2014).

The climate is primarily affected by the East-Asian Monsoon. In the cold/dry winter (from December to early March of the following year), the outer Changjiang Estuary is dominated by the monsoon-driven Yellow Sea Coastal Current (YSCC) and the CDW flows southward (Zhai, Chen, et al., 2014). In the warm/wet summer (from June to early September), the CDW flows northeastward and carries tremendous amounts of materials into the ECS (Chen, 2009; Figure 1b).

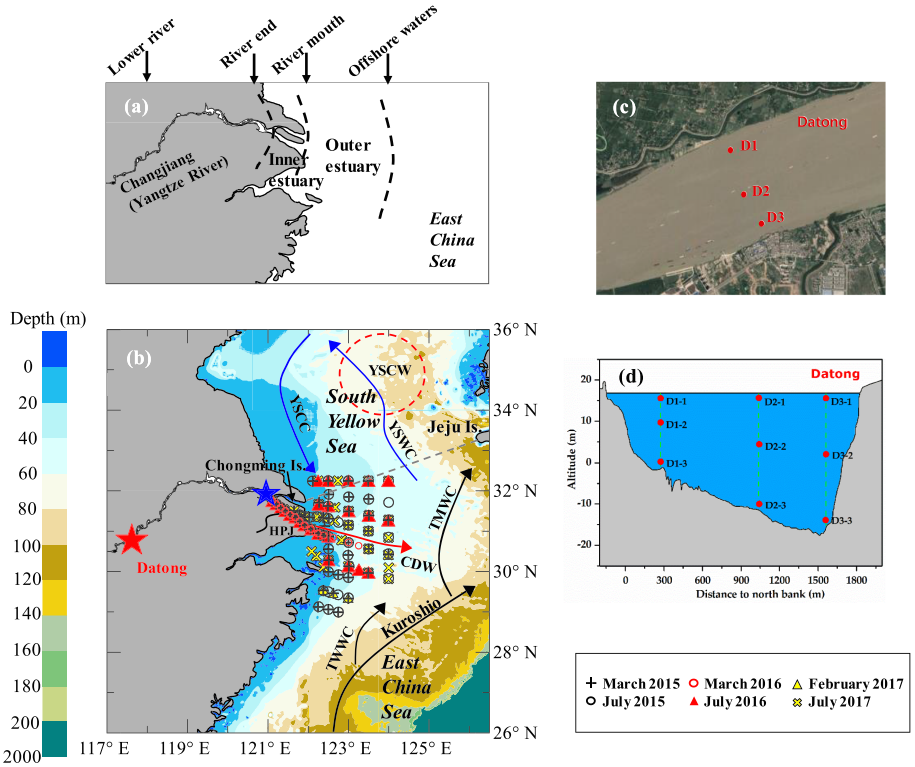


**Figure 1.** Maps showing (a) the continuum spanning from the lower Changjiang (Yangtze River) to the Changjiang Estuary, and to the adjacent East China Sea (ECS), and (b) sampling sites together with the circulation and depth contour in the ECS and the South Yellow Sea, and (c and d) the horizontal section and vertical samples at Datong Station. In the East China Sea and the South Yellow Sea (demarcated by a straight line from the north of the Changjiang Estuary to Jeju Island, Korea), major currents include the Kuroshio, TsushiMa Warm Current (TMWC) and Taiwan Warm Current (TWWC) existing throughout the year, and the Yellow Sea Coastal Current (YSCC) and Yellow Sea Warm Current (YSWC) in the northeast monsoon seasons. The Changjiang Diluted Water (CDW) and Yellow Sea Cold Water Mass (YSCW) appear during southwest monsoon seasons. The Datong Station and a sampling site at river end (west of Chongming Island) were marked using pentacles. HPJ = Huangpujiang River, which is the farthest downstream tributary of the Changjiang, collecting most runoffs from the metropolitan Shanghai.

## 2.2. Sampling and Analyses

To characterize monthly variations of the riverine transports of DIC and TAlk, 16 surveys were carried out at Datong Station, one in each month from May 2015 to August 2016 (Table 1), usually collecting nine water samples of different depths along a cross section (Figures 1c and 1d). During this period, mapping cruises were also conducted in March and July 2015, March and July 2016 and February and July 2017, sampling the Changjiang Estuary from its river end to the northwestern ECS (Figure 1b). To extend our temporal coverage, 16 previous estuarine/coastal mapping cruises (spanning different seasons in 2005–2012) and another inner-estuary survey (during 9–10 May 2017) were included in this study (Tables 2 and 3 and Figure 2).

During our estuarine mapping cruises in 2015–2017, water samples were collected at two or three different depths (including sea surface and the bottom water) using 5 or 30 L Niskin bottles. The ancillary data of in situ temperature were obtained using a calibrated Conductivity-Temperature-Depth/Pressure unit (SBE-19 plus, Sea Bird Co.) or a calibrated YSI6600 multi-parameter probe. Salinity (Practical Salinity Scale of 1978) was measured with a calibrated WTW's TetrCon®925 probe. The dissolved oxygen (DO) samples were collected, fixed, and titrated aboard following the classic Winkler procedure at the satisfactory level of <0.5%. A small quantity of $NaN_3$ was added during subsample fixation to remove possible interferences from nitrites (Wong, 2012). The DO saturation (DO%) was calculated from field-measured DO concentration divided by the DO concentration at equilibrium with the atmosphere which was calculated from temperature, salinity and local air pressure, as per the Benson and Krause (1984) equation. To quantify the effects of net community metabolism, apparent oxygen utilization (AOU) was also calculated by subtracting the

**Table 1**
*TAlk and DIC (Mean ± SD) at Datong Station and the Monthly Riverine Transport Fluxes in the Lower Changjiang River*

| Sampling date | Monthly water discharge ($m^3$/s) | TAlk (μmol/kg) | DIC (μmol/kg) | $F_{TAlk}$ (mol/s) | $F_{DIC}$ (mol/s) |
|---|---|---|---|---|---|
| 12 May 2015 | 30,943 | 1,931±10 (*n*=9) | 1,943±12 (*n*=9) | 59,563 | 59,943 |
| 12 June 2015 | 50,151 | 1,480 (*n*=1) | 1,485 (*n*=1) | 73,980 | 74,230 |
| 14 July 2015 | 49,488 | 1,671±16 (*n*=6) | 1,684±13 (*n*=6) | 82,453 | 83,082 |
| 17 August 2015 | 32,723 | 1,621±9 (*n*=6) | 1,628±12 (*n*=6) | 52,887 | 53,101 |
| 15 September 2015 | 30,375 | No data | 1,746±11 (*n*=9) | No data | 52,892 |
| 12 October 2015 | 26,911 | No data | 1,764±9 (*n*=9) | No data | 47,342 |
| 16 November 2015 | 26,078 | 1,761±7 (*n*=7) | 1,770±3 (*n*=7) | 45,781 | 46,010 |
| 11 December 2015 | 25,695 | 1,571±14 (*n*=9) | 1,609±15 (*n*=9) | 40,247 | 41,223 |
| 14 January 2016 | 21,082 | 1,694±14 (*n*=9) | 1,707±12 (*n*=9) | 35,606 | 35,873 |
| 17 February 2016 | 20,434 | 1,578±6 (*n*=6) | 1,585±4 (*n*=6) | 32,155 | 32,300 |
| 14 March 2016 | 21,227 | 1,734±11 (*n*=8) | 1,739±9 (*n*=8) | 36,699 | 36,811 |
| 11 April 2016 | 34,728 | 1,603±12 (*n*=6) | 1,615±16 (*n*=6) | 55,513 | 55,923 |
| 19 May 2016 | 47,053 | 1,509±10 (*n*=7) | 1,532±11 (*n*=7) | 70,780 | 71,891 |
| 16 June 2016 | 49,838 | 1,592±5 (*n*=7) | 1,617±16 (*n*=7) | 79,107 | 80,340 |
| 13 July 2016 | 65,622 | 1,734±18 (*n*=6) | 1,756±27 (*n*=6) | 113,456 | 114,910 |
| 18 August 2016 | 51,026 | 1,751±10 (*n*=9) | 1,778±10 (*n*=9) | 89,099 | 90,462 |

field-measured DO concentration from the air-equilibrated DO. Assuming the water starts with a fully saturated state, and ignoring immediate effects of air-sea exchange and water mixing, an AOU > 0 implies net community respiration, while an AOU < 0 implies net community production.

Seawater samples (out of 122°E, usually with Salinity of > 10) for DIC and TAlk analyses were stored in 60-ml borosilicate glass bottles (bubble free) and 140-ml high-density polyethylene bottles, respectively. They were immediately mixed with 50 μl of saturated $HgCl_2$, and then sealed and preserved at room temperature until determination. According to Huang et al. (2012), there were no statistical differences for seawater samples between the measuring results from our procedure and from those stored in the borosilicate glass bottles suggested by Dickson et al. (2007). The freshwater, or low-salinity samples (Salinity < 10), were stored in 250-ml Teflon coated glass bottles (Corning Pyrex®, Corning Inc., USA) together with ground-glass stoppers, mixed with 200 μl of saturated $HgCl_2$. According to a parallel storage technique study conducted in our 2015 surveys, these Teflon-coated glass bottles are suitable for relatively long-term (~70 days) storage of freshwater carbonate samples (Liu & Zhai, 2016).

DIC and TAlk data were collected by commercial analytical systems (Model AS-C3 and AS-ALK1+, Apollo SciTech Inc., USA). Following Cai (2003) and Zhai et al. (2007), DIC was measured by infrared detection following acid extraction of a 0.5- to 0.9-ml sample with a Kloehn® digital syringe pump, and TAlk was determined at 25 °C by Gran acidimetric titration on a 15- to 25-ml sample with a Kloehn® digital syringe pump, using a precision pH meter and an Orion® 8102BN Ross electrode for detection. Both DIC and TAlk determinations were referred to Certificated Reference Materials (CRM) from Andrew G. Dickson's lab at Scripps Institute of Oceanography at a precision of ± 2 μmol/kg (Dickson et al., 2007; Zhai et al., 2007).

### 2.3. Flux Estimation

We daily collected the Datong Station water discharge data (Figure 2a) from China Bureau of Hydrology (http://xxfb.mwr.cn/ssIndex.html) and/or Changjiang Water Resources Commission, China (http://www.cjh.com.cn/). The daily discharge data were summed up to obtain weekly, monthly and yearly water discharges from the river to the estuary over the study period. Based on an in-situ study conducted in the Changjiang Estuary, there is no significant difference between the water discharges at Datong Station and those at the river end of the estuary (Wang, Pan, et al., 2006). Assuming TAlk and DIC concentrations remained in a steady state during the month under investigation, as evidenced by our earlier results showing that TAlk and DIC values in the river-end only varied less than 4% within each month (Zhai et al., 2007), the monthly averaged transport fluxes ($F$) were estimated via TAlk and DIC concentrations multiplied by relevant monthly averaged water discharges ($Q$). To detect the sensitivity of short-term variations in water discharges on flux estimations, the weekly and monthly averaged fluxes were calculated via TAlk and DIC concentrations multiplied by the weekly and monthly averaged water discharge, respectively. The

**Table 2**
*TAlk and DIC (Mean ± SD) at the River-End (West of Chongming Island) and Monthly Riverine Transport Fluxes Into the inner Changjiang Estuary*

| Sampling dates | Monthly water discharge ($m^3$/s) | TAlk (μmol/kg) | DIC (μmol/kg) | $F_{TAlk}$ (mol/s) | $F_{DIC}$ (mol/s) |
|---|---|---|---|---|---|
| 6–7 October 2005 | 31,320 | 1,712±13 ($n$=6) [a] | 1,727±18 ($n$=6) [a] | 53,474 | 53,917 |
| 26–29 December 2005 | 13,981 | 1,952±13 ($n$=22) [a] | 1,968±18 ($n$=22) [a] | 27,214 | 27,440 |
| 6–7 April 2006 | 24,200 | 1,639±36 ($n$=15) [a] | 1,640±36 ($n$=15) [a] | 39,543 | 39,571 |
| 13 April 2007 | 17,141 | 1,591±9 ($n$=10) | No data | 27,194 | No data |
| 13 October 2007 | 25,992 | 1,781±18 ($n$=3) | No data | 46,155 | No data |
| 15 December 2008 | 17,036 | 1,755±2 ($n$=2) | 1,758±7 ($n$=2) | 29,810 | 29,861 |
| 12 April 2009 | 22,898 | 1,691±1 ($n$=2) | 1,710±2 ($n$=2) | 38,605 | 39,039 |
| 15 April 2010 | 30,427 | 1,495 ($n$=1) [b] | 1,520 ($n$=1) [b] | 45,354 | 46,112 |
| 11 January 2011 | 15,431 | 1,592 ($n$=1) | 1,600 ($n$=1) | 24,494 | 24,617 |
| 15 April 2011 | 16,020 | 1,846±5 ($n$=4) | 1,888±4 ($n$=4) | 29,486 | 30,152 |
| 19 July 2011 | 36,873 | 1,710±12 ($n$=3) | 1,761±25 ($n$=3) | 62,866 | 64,725 |
| 18 October 2011 | 20,773 | 1,735±10 ($n$=2) | 1,760±10 ($n$=2) | 35,935 | 36,453 |
| 16 February 2012 | 15,551 | 1,722 ($n$=1) | 1,784 ($n$=1) | 26,700 | 27,665 |
| 15 March 2015 | 20,802 | 1,782±1 ($n$=2) [c] | 1,805±3 ($n$=2) [c] | 36,966 | 37,431 |
| 09 July 2015 | 49,488 | 1,734±7 ($n$=2) [c] | 1,762±5 ($n$=2) [c] | 85,549 | 86,955 |
| 11 March 2016 | 21,227 | No data | 1,865±26 ($n$=2) | No data | 39,464 |
| 5 July 2016 | 65,622 | 1,707±7 ($n$=2) | 1,775±7 ($n$=2) | 111,712 | 116,157 |
| 19–23 February 2017 | 13,335 | 1,874±15 ($n$=4) | 1,883±14 ($n$=4) | 24,918 | 25,033 |
| 9–10 May 2017 | 29,143 | 1,698±11 ($n$=4) | 1,750±11 ($n$=4) | 49,343 | 50,856 |
| 21 July 2017 | 58,510 | 1,554±28 ($n$=4) | 1,590±18 ($n$=4) | 90,635 | 92,757 |

[a]These data were from Zhai et al. (2007). [b]These data were from Zhai et al. (2017). [c]These data were from Liu and Zhai (2016).

comparison results suggested that there were no significant differences between the fluxes based on the monthly averaged water discharge and those based on the weekly averaged water discharge (TAlk, $R^2$ = 0.985, $p < 0.001$; DIC, $R^2 = 0.984$, $p < 0.001$; Figure S1 in the supporting information).

In order to extend flux time-series, we plotted $F$ against $Q$ to obtain a simplified relationship between monthly flux and water discharge, as equation (1):

$$F = a \times Q \quad (1)$$

where $a$ represents discharge-weighted mean concentration. The yearly fluxes are determined by summing up all the 12 monthly data in a whole year.

To evaluate the net effect of estuarine processes on the carbonate fluxes, we calculated the estuarine TAlk and DIC export fluxes to the sea using the effective concentration method (Cai et al., 2004; Officer, 1979). The effective TAlk and DIC concentrations for the estuarine export flux estimation were obtained by extrapolating data-based conservative mixing lines of TAlk and DIC from the high-salinity area to zero salinity (Cai et al., 2004). The differences between the effective TAlk and DIC concentrations and measured TAlk and DIC concentrations at the river end-member indicated the additions or removals of TAlk and DIC in the estuary (Boyle et al., 1974; Cai & Wang, 1998; Officer, 1979). Then the effective TAlk and DIC concentrations were multiplied by the water discharge from the Changjiang River to get the estuarine export fluxes to the sea.

### 2.4. Calculation of Other Carbonate System Parameters From TAlk and DIC

The partial pressure of $CO_2$ ($pCO_2$), $pH_T$ (the negative logarithm of the total concentration of $H^+$ and $HSO_4^-$ ions) and $\Omega_{arag}$ were calculated from temperature, salinity, and measured DIC and TAlk using the software CO2SYS.XLS (Version 24; Pelletier et al., 2015), which is an updated version of the original CO2SYS.EXE (Lewis & Wallace, 1998). The Millero et al. (2006) dissociation constants of carbonic acid were used in the calculation due to their broad applicability with ranges of temperature (0–50 °C) and salinity (0–50). The Dickson (1990) dissociation constant was used for $HSO_4^-$ ion. The phosphate and silicate values required by the program were unavailable and replaced by zero. According to Lukawska-Matuszewska (2016), this simplification may result in an underestimation of non-carbonate inorganic alkalinity of tens of μmol/kg in low-salinity area, under the present-day silicate level of ~100 μmol/kg and phosphate level

**Table 3**
*Effective Values of TAlk and DIC Concentrations at River End-Member and the Monthly Estuarine Export Fluxes From the Changjiang Estuary to the Sea*

| Sampling dates | Monthly water discharge ($m^3$/s) | TAlk (μmol/kg) | DIC (μmol/kg) | $F_{TAlk}$ (mol/s) | $F_{DIC}$ (mol/s) |
|---|---|---|---|---|---|
| 24–26 December 2005 and 01 January 2006 | 13,981[a] | 1,970 | 2,000 | 27,462 | 27,880 |
| 8–27 April and 2–7 May 2007 | 17,141[a] | 1,825 | 1,830 (1200[b]) | 31,190 | 31,275 (4,307[c]) |
| 7–9 November 2007 | 25,992 | 1,830 | 1,860 | 47,425 | 48,203 |
| 6–13 April 2009 | 22,898 | 1,700 | 1,730 (900[b]) | 38,811 | 39,496 (4,993[c]) |
| 12–20 June 2010 | 50,357 | 1,600 | 1,670 (1,200[b]) | 80,334 | 83,848 (9,203[c]) |
| 1–10 November 2010 | 17,876 | 1,800 | 1,850 | 32,081 | 32,972 |
| 8–13 April 2011 | 16,020 | 2,020 | 2,050 | 32,266 | 32,745 |
| 7–22 July 2011 | 36,873 | 1,760 | 1,790 (900[b]) | 64,704 | 65,807 (6,644[c]) |
| 17–21 October 2011 | 20,773 | 1,900 | 1,915 | 39,353 | 39,664 |
| 2–3 May 2012 | 42,243 | 1,610 | 1,640 (1,200[b]) | 67,811 | 69,074 (7,413[c]) |
| 11–21 March 2015 | 20,802 | 2,100 | 2,145 | 43,555 | 44,488 |
| 9–20 July 2015 | 49,488 | 1,705 | 1,735 (850[c]) | 84,129 | 85,609 (7,652[c]) |
| 11–17 March 2016 | 21,227 | 1,720 | 1,800 | 36,402 | 38,095 |
| 4–15 July 2016 | 65,622 | 1,705 | 1,735 (800[b]) | 111,556 | 113,519 (22,973[c]) |
| 20–31 July 2017 | 58,510 | 1,570 | 1,600 (1,000[c]) | 91,589 | 93,339 (9,293[c]) |

[a]Averaged water discharge in the first month of the sampling period. [b]Specific effective concentrations at zero salinity considering the biological drawdown of DIC ($C_0^*{}_{bio}$ in section 4.3). [c]Biological-production-induced flux loss in the outer estuary ($L_{bio}$ in section 4.3).

of 1–2 μmol/kg in the Lower Changjiang (e.g., Zhai et al., 2017). This is why the calculation results at salinity <10 are uncertain. The $Ca^{2+}$ concentrations were assumed to be proportional to salinity as presented in Millero (1979) and the values of apparent solubility product for aragonite ($K_{sp}^*{}_{arag}$) were taken from Mucci (1983).

To assess the quality of the carbonate system data, we also calculated pH data using the National Bureau of Standards (NBS) scale based on DIC and TAlk values. These data were compared with field-measured pH data (also obtained using the NBS scale). Most measured and calculated values at salinity of > 10 were significantly consistent with each other ($R^2 = 0.985$, $p < 0.001$), suggesting that measurements of the carbonate system parameters were reliable (Figure S2).

## 3. Results

### 3.1. Hydrological Settings

Water discharge of Changjiang was recorded at $9.06 \times 10^{11}$ $m^3$/year at Datong Station in 2015, which was nearly the same as the long-term average of $9.03 \times 10^{11}$ $m^3$/year over the period of 1963–1999 (Liu et al., 2002) before the building of Three Gorges Dam. In 2016, however, its annual water discharge reached $10.41 \times 10^{11}$ $m^3$/year, representing the highest annual water discharge since the Three-Gorges Dam's completion. Such dramatic flooding is presumably due to the strong El Niño-Southern Oscillation (ENSO) event in 2015–2016 (Mei et al., 2018).

The hydrology of Lower Changjiang was characterized by a single water discharge peak in July (Figure S3). Thus, our February–March cruises (with relatively low water discharge of $2.08 \times 10^4$ $m^3$/s in March 2015, $2.12 \times 10^4$ $m^3$/s in March 2016 and $1.33 \times 10^4$ $m^3$/s in February 2017) represented the end of the dry season, while our July cruises (with high water discharge values of $4.95 \times 10^4$ $m^3$/s in July 2015, $6.56 \times 10^4$ $m^3$/s in July 2016 and $5.85 \times 10^4$ $m^3$/s in July 2017) represented the flood season.

In the inner Changjiang Estuary (west of 122°E), the water column was well mixed at almost all stations. The early spring water temperature was ~11 °C in March of 2015–2016 and 8–10 °C in February 2017 (Figure 3a). The summertime water temperature was ~26 °C in July of 2015–2016 and ~29 °C in July 2017 (Figure 3f). The wintertime salinity was 0.16–0.87 in March of 2015–2016 in the inner estuary. In February 2017, however, relatively high salinity of 4–14 was observed at two stations close to the riverine mouth at 122°E (Figure 3b). Summertime salinity was always lower than 0.2 in the inner estuary during our three July cruises (Figure 3g). The early spring DO was nearly in equilibrium with the atmosphere, while the summertime DO was undersaturated (~75%; Figures 3c and 3h).

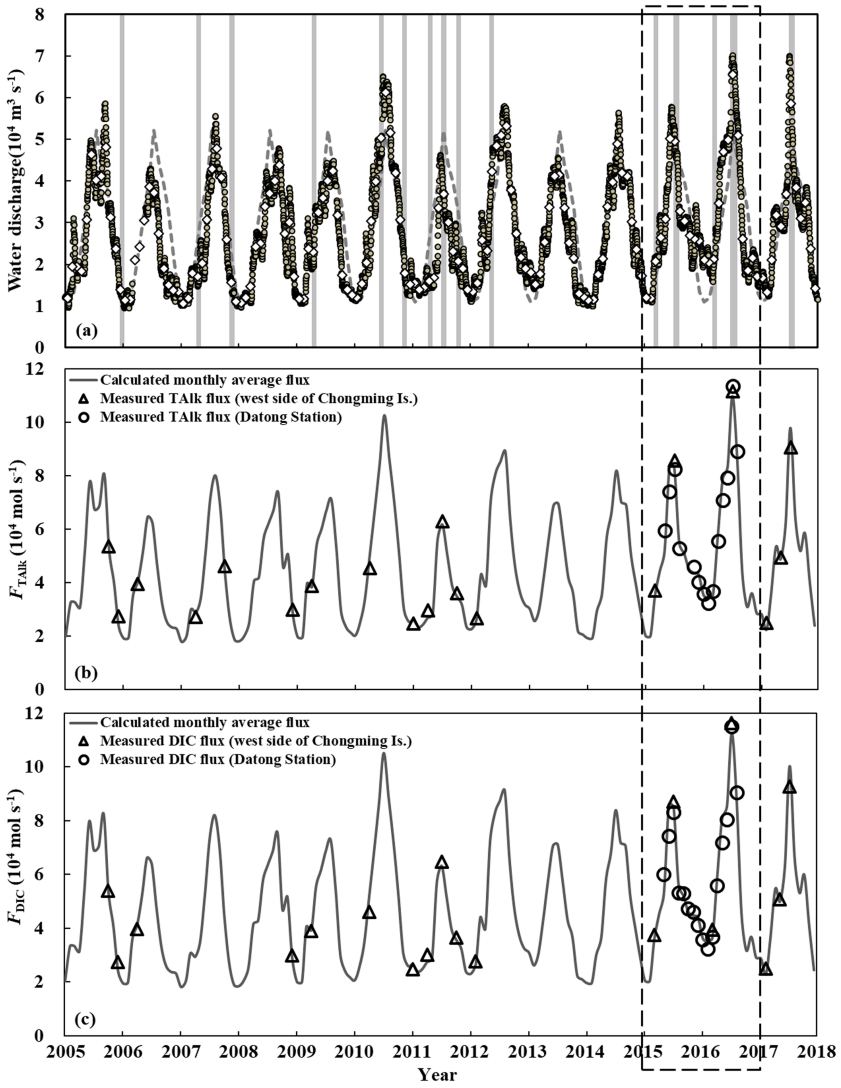


**Figure 2.** (a) Evolution of water discharge at Datong Station from 2005 to 2017 and (b and c) Changjiang monthly fluxes of total alkalinity (TAlk) and dissolved inorganic carbon (DIC). Water discharge data are from China Bureau of Hydrology (now at http://xxfb.mwr.cn/ssIndex.html) and/or Changjiang Water Resources Commission (http://www.cjh.com.cn/). In panel (a), the gray dashed curve shows the long-term average of monthly water discharge during 1963–1999 (Liu et al., 2002). Gray vertical lines show sampling periods of our 15 mapping cruises in the outer Changjiang Estuary, including those surveys described by Zhai et al. (2007); Zhai, Chen, et al., 2014), Zhai and Hong (2012), Liu and Zhai (2016), and Zhai (2018). In panels (b) and (c), the gray solid lines represent the calculated TAlk and DIC fluxes based on equations (10) and (11), respectively. The open circles show data at Datong Station and the open triangles indicate the river-end data at the site west of Chongming Island.

The outer Changjiang Estuary was vertically well-mixed at most stations during our early spring cruises of 2015–2017. The water temperature ranged from 7.7 to 15.8 °C and the salinity ranged from 7.72 to 34.78 in the outer estuary (Figures 3a and 3b). A significant salinity front was observed around ~122.5°E where freshwater mixed with sea waters, and the CDW with salinity <31 occupied the west of 123°E. The lowest water temperatures of 6.6–8.8 °C (with salinity values of 31.2–32.4) were measured at several northwest stations. The nearly air-equilibrated DO (DO% ranging between 91% and 111%) in whole water columns indicated again the strong vertical water mixing and air-sea exchange compared to biological processes (Figure 3c).

In July, strong water column stratification occurred in the outer estuary (Figures 3f–3h) owing to sea surface heating and freshwater intrusion. The surface water temperature ranged from 20.5 to 30.9 °C and the bottom water temperature ranged from 18.5 to 28.3 °C. The salinity front was also observed around the estuary

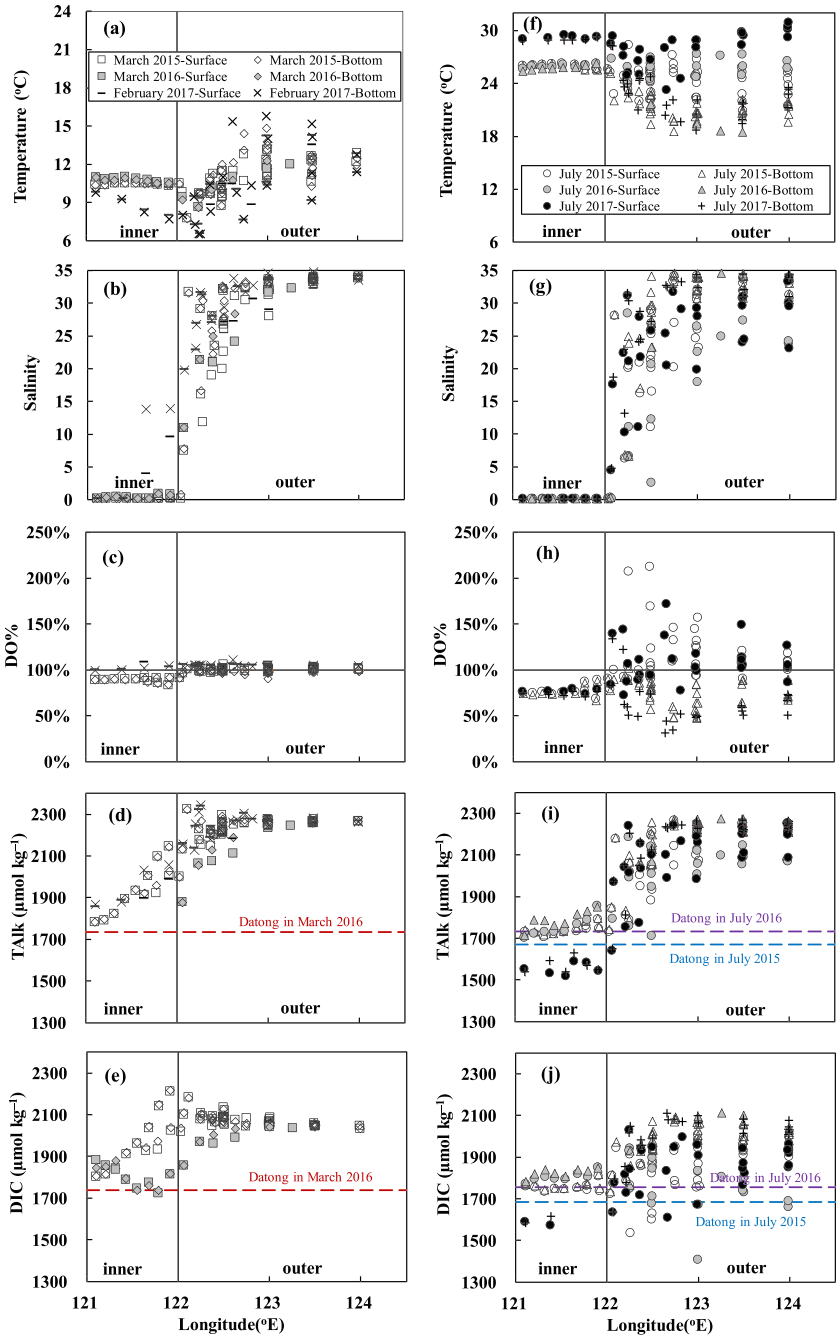


**Figure 3.** Flow-path distributions of (a and f) water temperature, (b and g) salinity, (c and h) DO saturation, (d and i) total alkalinity (TAlk), and (e and j) dissolved inorganic carbon (DIC) in the Changjiang Estuary in late spring and summer. Some of our 2015 data have been published by Liu and Zhai (2016). The vertical line indicates the boundary along 122°E between the inner and outer parts of the Changjiang Estuary (Zhai et al., 2007). In panels (d), (e), (i), and (j), dashed horizontal lines represent the Datong Station TAlk and DIC concentrations obtained in the relevant month.

mouth of ~122.5°E, while the CDW with salinity <31 extended to 123.4°E in July 2015 and even 124°E during the July 2016–2017. High sea surface DO% values of 120% to 212% were measured at most stations, showing significant biological production in the surface water of the outer estuary. The bottom-water DO % (from 32% to 90%), however, were lower than the air-equilibrated level, indicating the domination of oxygen-depletion processes.

### 3.2. TAlk and DIC in the Changjiang Estuary and Beyond

At Datong Station, TAlk varied between 1,480 and 1,931 μmol/kg from May 2015 to August 2016, while DIC was measured at 1,485–1,943 μmol/kg, slightly higher than TAlk over the survey period (Table 1). To examine monthly variations, we plotted TAlk and DIC concentrations at Datong Station (survey-averaged values with relative standard deviation values of <1%) versus corresponding water discharges (Figures 4a and 4b). Unlike the historical monthly variations of TAlk and DIC concentrations (Liu et al., 2002) before the Three Gorges Dam was built, our TAlk and DIC concentrations in dry seasons (from October to March of the next year) were similar to those obtained in the flood season (from June to September; Figures 4a and 4b). Significantly, present-day TAlk and DIC concentrations in dry seasons were lower than the historical long-term average values (Figure S4), presumably due to dry-season water retention of the Three Gorges Dam. It is worth noting that the upper Changjiang waters contain a high level of the weathering product TAlk (Wu et al., 2007; Zhang et al., 2014).

In the inner Changjiang Estuary, TAlk increased from 1,782 μmol/kg at a site west of Chongming Island (~121°E) to 2,148 μmol/kg at a site near the river mouth (~122°E), while DIC rose from 1,803 μmol/kg at the west site (~121°E) to 2,212 μmol/kg near the river mouth (~122°E) during our early spring cruises (Figures 3d and 3e). DIC values in March 2016 varied between 1,724 and 1,883 μmol/kg in the inner estuary, where low DIC values of 1,724–1,775 μmol/kg were observed in the central area of the inner estuary. The dynamic changes of TAlk and DIC in the inner estuary were likely subject to insufficient water mixing, resulted from the limited residence time (e.g., 7–8 days in spring, Zhai et al., 2017) and numerous local water sources such as the Huangpujiang River input (Figure 1b; Zhai et al., 2007) and spillover fluxes from the North Branch (Zhai et al., 2017). Such intra-monthly dynamics were unresolved in this study. During July cruises, TAlk and DIC varied limitedly along the longitude in the inner estuary (Figures 3i and 3j). The summertime values of TAlk and DIC were slightly lower than those obtained in our February-March cruises, presumably due to the dilution effect of rainwater in wet seasons. Most TAlk and DIC concentrations at the site west of Chongming Island (~121°E) were slightly higher than those obtained at Datong Station during the same study period.

In the outer Changjiang Estuary, TAlk and DIC were plotted against salinity (Figure 5). During our early spring cruises (February–March in 2015–2017), most data were linearly related to the salinity (Figures 5a and 5b). In March 2015, TAlk ranged from 2,000 to 2,327 μmol/kg and DIC varied-between 2,020 and 2,183 μmol/kg. Several very high TAlk values of 2,292–2,327 μmol/kg were observed at two northwest stations during the March 2015 cruise (with a salinity range of 31.6–32.4), indicating the effect of monsoon-driven YSCC (with higher DIC and TAlk) intrusion, as previously reported by Zhai, Chen, et al. (2014) in this region. In March 2016, TAlk and DIC ranged from 1,877 to 2,257 μmol/kg and from 1,856 to 2,043 μmol/kg in the outer estuary, respectively. In February 2017, TAlk varied between 2,034 and 2,345 μmol/kg. Extremely high TAlk values of >2,300 μmol/kg were also observed at those northwest stations. The different relationship between carbonate parameters and salinity observed in March 2015, March 2016 and February 2017 (Figures 5a and 5b) suggested that the freshwater end-member values of TAlk and DIC of the CDW were subject to inter-annual variations.

During our July cruises, TAlk ranged from 1,752 to 2,274 μmol/kg and DIC was from 1,407 to 2,110 μmol/kg in the outer estuary (Figures 5e and 5f). TAlk still showed tight relationships with salinity. However, DIC exhibited a much weaker relationship with salinity in summer, since DIC variation is subject to alteration of primary production (related to DIC removal) and respiration and/or remineralization (related to DIC addition). Most sea surface DIC values were lower than 1,900 μmol/kg, likely due to the summertime net community production in this region. This was evidenced by very high sea surface DO% of 120–212% in the CDW in summer. In contrast, very high DIC values of >2,050 μmol/kg in bottom waters was associated with quite low DO% values of <75%, showing the effects of net community respiration and/or remineralization. It is worth noting that typically seawater DIC:TAlk ratio of 0.84–0.94 was revealed in ECS offshore waters (salinity >31), which was substantially lower than the riverine DIC:TAlk ratio of >1 as shown in Table 2.

In July 2015 and 2017, conservative water mixing lines of TAlk versus salinity were fitted based on field data with salinity >10, as equations (2) and (3):

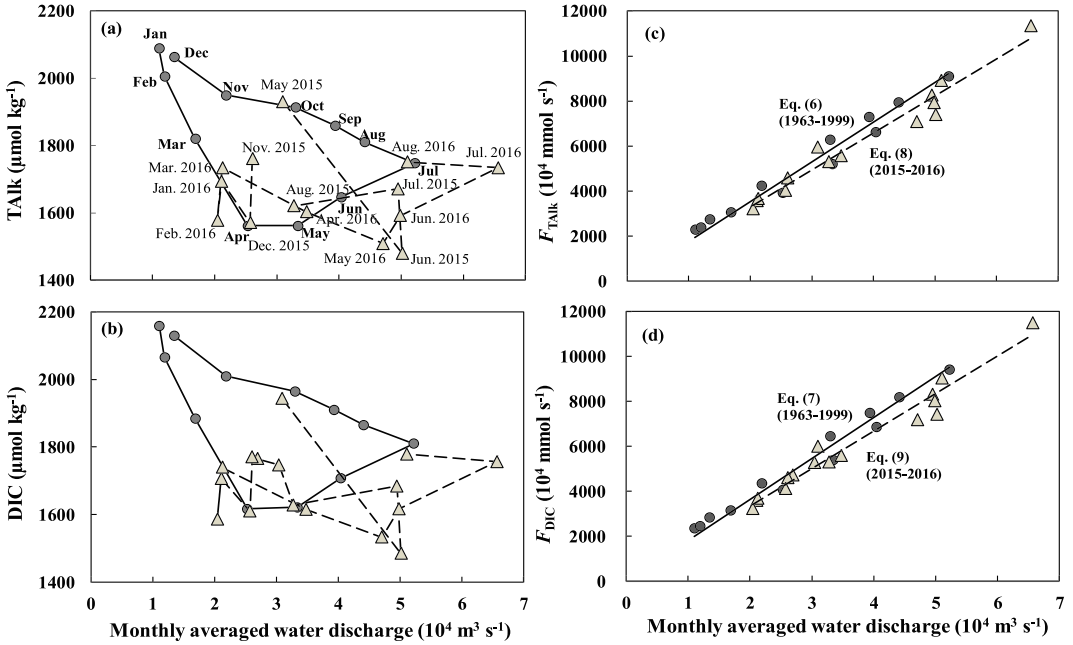


**Figure 4.** Monthly averaged concentrations of (a and b) total alkalinity (TAlk) and dissolved inorganic carbon (DIC) versus water discharge and (c and d) the riverine transport fluxes versus the water discharge at Datong Station. In panels (a) and (b), circles connected with solid lines indicate historical long-term averaged monthly values (Liu et al., 2002), and triangles connected with dashed lines represent data collected in this study (Table 1). The historical monthly variations have been discussed by Zhai et al. (2007). In panels (c) and (d), the solid and dashed lines show relationships in 1963–1999 and in 2015–2016, respectively.

$$\mathrm{TAlk}^{\mathrm{conservative\_in\_July2015}}\ (\ \mu\mathrm{mol/kg}) = 16.09\times\mathrm{salinity} + 1705\ \left(R^2 = 0.97, n = 119\right) \quad (2)$$

$$\mathrm{TAlk}^{\mathrm{conservative\_in\_July2017}}\ (\ \mu\mathrm{mol/kg}) = 20.54\times\mathrm{salinity} + 1570\ \left(R^2 = 0.98, n = 78\right) \quad (3)$$

TAlk data of our July 2016 cruise also followed equation (2), except for two nearshore TAlk values (1,945–1,992 μmol/kg at salinity 11 and 12) that were higher than predicted values from salinity. They were obtained at two stations around 122.3°E 31.6°N, where salt marsh developed and likely releasing dissolved inorganic elements to overlying waters (Zhai et al., 2017). The freshwater end-members of TAlk and DIC in July 2017 were lower than those in 2015 and 2016 (see water mixing lines in Figures 5e and 5f). Extrapolating equations (2) and (3) to the highest salinity of 34.56 during our surveys, the TAlk values of ECS offshore waters were estimated at 2261 (in 2015 and 2016) and 2280 (in 2017) μmol/kg. Both were comparable with the TAlk value of the Kuroshio Tropical Water, that is, 2,293 μmol/kg at a salinity of 34.9 (Chen & Wang, 1999), suggesting that the relevant ECS offshore waters observed in this study may originate from Kuroshio surface waters as earlier illustrated by Chen et al. (1995) and recently by Zhai, Chen, et al. (2014).

DIC is not a conservative parameter. In this study, the riverine end-member value of DIC was assumed to be 30 μmol/kg higher than that of TAlk (Guo et al., 2012). A sampling site with salinity of 33.82 and DO% of 102.8% (DIC = 1,963 μmol/kg) during our July 2015 cruise was adopted to calculate the offshore seawater end-member. Then we established a conservative water mixing line of DIC versus salinity as follow:

$$\mathrm{DIC}^{\mathrm{conservative\_in\_July2015}}\ (\ \mu\mathrm{mol/kg}) = 6.74\times\mathrm{salinity} + 1735 \quad (4)$$

$$\mathrm{DIC}^{\mathrm{conservative\_in\_July2017}}\ (\ \mu\mathrm{mol/kg}) = 11.25\times\mathrm{salinity} + 1600 \quad (5)$$

From the above equations, relevant riverine $pCO_2$ could be calculated at 1,174 μatm (at 26 °C) in 2015 and 1,209 μatm (at 28 °C) in 2017, similar to the field-measured values (1105±70 μatm at 28°C in August 2003) in the inner Changjiang Estuary (Chen et al., 2008; Zhai et al., 2007). Extrapolating equations (2)–(5) to a

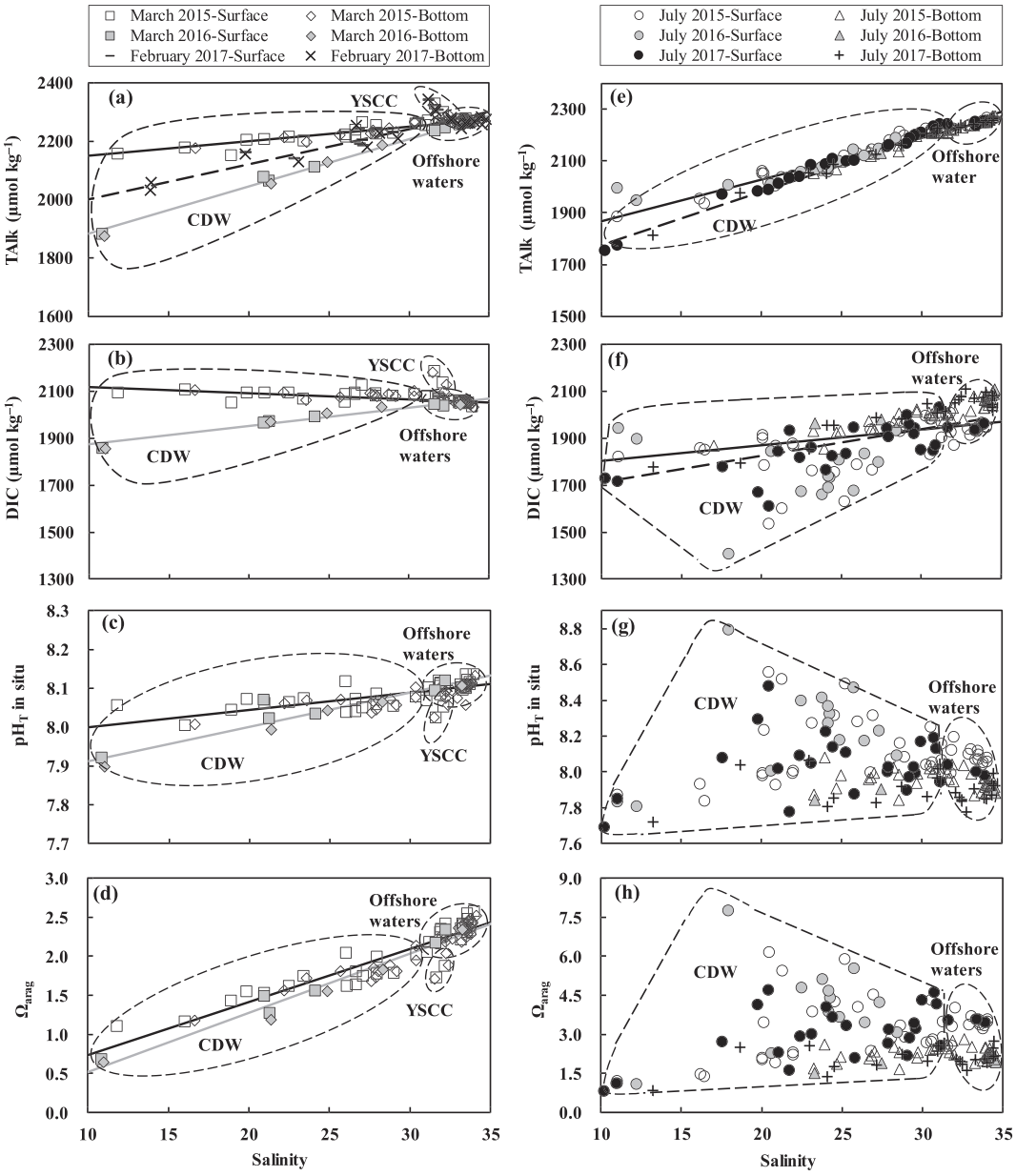


**Figure 5.** Carbonate parameters versus salinity in the outer Changjiang Estuary in spring (a–d) and summer (e–h) during 2015–2017. YSCC = Yellow Sea Coastal Current, CDW = Changjiang Diluted Water. The assumed water mixing lines of TAlk and DIC in the CDW refer to equations (2)–(5).

salinity of 33.8–34.0, the ECS offshore waters had $pCO_2$ values of 392–400 μatm at the usual offshore surface temperature of ~25 °C, which was similar to the air-equilibrated level (390–400 μatm).

### 3.3. TAlk and DIC Fluxes

The monthly riverine TAlk and DIC transport fluxes in the lower Changjiang River from May 2015 to August 2016 were calculated as shown in Table 1. Despite the regime shift of seasonal variations in TAlk and DIC during the past 55 years (Figures 4a and 4b), significant positive correlations between monthly riverine fluxes and water discharges were quite stable (Figures 4c and 4d). This is because the variation in water discharge was usually much larger than variations in TAlk and DIC concentrations. The relationships between the monthly riverine transport fluxes of TAlk ($F_{TAlk}$) and DIC ($F_{DIC}$) and water discharge ($Q$) at Datong

Station in 1963–1999 were established based on data reported by Liu et al. (2002), as equations (6) and (7). Similarly, relationships between $Q$ and fluxes in 2015–2016 were equations (8) and (9).

$$F_{\mathrm{TAlk}}{}^{\mathrm{Datong1963-1999}} = 1,763\ \ \mu\mathrm{mol/L}\times Q\ \left(R^2 = 0.97, n = 12\right) \quad (6)$$

$$F_{\mathrm{DIC}}{}^{\mathrm{Datong1963-1999}} = 1,819\ \ \mu\mathrm{mol/L}\times Q\ \left(R^2 = 0.97, n = 12\right) \quad (7)$$

$$F_{\mathrm{TAlk}}{}^{\mathrm{Datong2015-2016}} = 1,646\ \ \mu\mathrm{mol/L}\times Q\ \left(R^2 = 0.96, n = 14\right) \quad (8)$$

$$F_{\mathrm{DIC}}{}^{\mathrm{Datong2015-2016}} = 1,670\ \ \mu\mathrm{mol/L}\times Q\ \left(R^2 = 0.96, n = 16\right) \quad (9)$$

At Datong Station, the discharge-weighted mean concentrations of TAlk and DIC in 2015–2016 were 7–8% lower than historical long-term average in 1963–1999 (Figures 4c and 4d). By summing up all monthly fluxes over a year, the yearly riverine TAlk and DIC transport fluxes in the lower Changjiang River were $1.49 \times 10^{12}$ mol/year and $1.51 \times 10^{12}$ mol/year in 2015, respectively. The riverine TAlk and DIC transport fluxes in 2016 were estimated at $1.71 \times 10^{12}$ mol/year and $1.74 \times 10^{12}$ mol/year, respectively. About 67% of the fluxes occurred in wet seasons (from April to September), while the other 33% appeared in dry seasons (from October to March of the next year).

The river-end TAlk and DIC (at the estuarine site west of Chongming Island) were summarized based on a decadal dataset of 20 field cruises over 2005–2017 (Table 2). We established quantitative relationships between monthly riverine transport fluxes into the estuary and $Q$, as equations (10) and (11):

$$F_{\mathrm{TAlk}}{}^{\mathrm{RiverEnd2005-2017}} = 1,673\ \ \mu\mathrm{mol/L}\times Q\ \left(R^2 = 0.99, n = 19\right) \quad (10)$$

$$F_{\mathrm{DIC}}{}^{\mathrm{RiverEnd2005-2017}} = 1,714\ \ \mu\mathrm{mol/L}\times Q\ \left(R^2 = 0.99, n = 18\right) \quad (11)$$

The TAlk and DIC discharge-weighted mean concentrations at river-end over 2005–2017 were slightly higher (~2%) than those obtained at Datong Station. The calculated monthly transport fluxes matched the field-measured results with the averaged difference of 5%, suggesting that the carbonate increases along the riverine transport were insignificant from Datong Station to Chongming Island.

In 2005–2017, annual mean fluxes of $(1.44 \pm 0.20) \times 10^{12}$ mol TAlk/year and $(1.48 \pm 0.21) \times 10^{12}$ mol DIC/year were transported into the Changjiang Estuary, which were 8–9% lower than the historical long-term mean values of $(1.58 \pm 0.21) \times 10^{12}$ mol TAlk/year and $(1.63 \pm 0.22) \times 10^{12}$ mol DIC/year (Liu et al., 2002). Our decadal flux results were also slightly lower than another five-year (1997–2001) averaged $HCO_3^-$ flux of $1.53 \times 10^{12}$ mol/year at a sampling site ~180 km upstream to the river mouth of Changjiang (Li & Zhang, 2003) and a riverine DIC flux of $1.54 \times 10^{12}$ mol/year in 2005–2006 (Zhai et al., 2007). Excluding the extreme droughts in 2006 and 2011 (having water discharge values of ~75% of the past long-term average), the annual averaged riverine TAlk and DIC fluxes were $1.50 \times 10^{12}$ mol/year and $1.54 \times 10^{12}$ mol/year in the recent decade, which were still lower than Liu et al. (2002) historical results by 5–6%.

To obtain the estuarine export fluxes to the sea, effective TAlk and DIC concentrations were extracted by extrapolating data-based conservative mixing lines from the high-salinity area to zero salinity (Table 3 and Figures 6 and 7), following procedures described earlier by Cai et al. (2004), Guo et al. (2008), and Joesoef et al. (2017). The relationships between monthly estuarine TAlk and DIC export fluxes and $Q$ in 2005–2017 were established as equations (12) and (13):

$$F_{\mathrm{TAlk}}{}^{\mathrm{Export2005-2017}} = 1,687\ \ \mu\mathrm{mol/L}\times Q\ \left(R^2 = 0.98, n = 15\right) \quad (12)$$

$$F_{\mathrm{DIC}}{}^{\mathrm{Export2005-2017}} = 1,721\ \ \mu\mathrm{mol/L}\times Q\ \left(R^2 = 0.98, n = 15\right) \quad (13)$$

The estuarine TAlk and DIC export fluxes from the Changjiang Estuary into the sea were averaged at $(1.46 \pm 0.20) \times 10^{12}$ mol/year and $(1.49 \pm 0.21) \times 10^{12}$ mol/year over the period of 2005–2017, representing the second highest carbonate dischargers in the world (Figure S5) after the Amazon ($2.4 \times 10^{12}$ mol/year; Cai et al., 2008) and accounts for ~4.5% of the total riverine DIC flux in the world ($33 \times 10^{12}$ mol/year, Bauer et al., 2013). As summarized in Table 4, the discharge-weighted mean concentrations of TAlk and DIC at river-

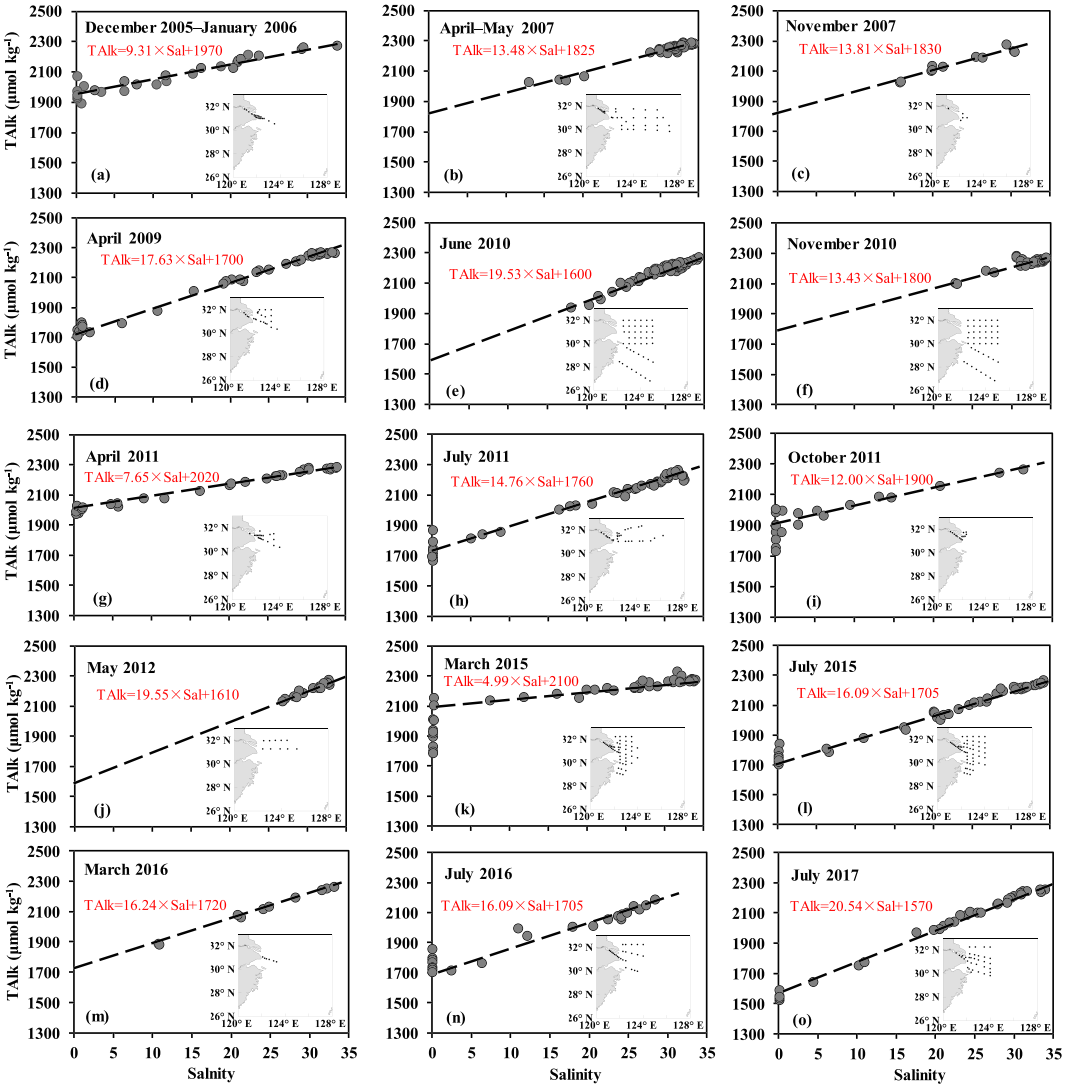


**Figure 6.** Sea surface total alkalinity (TAlk) versus salinity in the outer Changjiang Estuary during 2005–2017. Data in late 2005 and early 2006 are from Zhai et al. (2007), while data in 2007 are from Zhai and Hong (2012) and Zhai, Chen, et al. (2014). Data in May 2012 are from Zhai (2018), while data in 2015 have been partially published by Liu and Zhai (2016). Insert panels show sampling sites. Broken lines together with equations are the assumed conservative water mixing lines.

end in 2005–2017 were 5–6% lower than the historical long-term average in 1963–1999. The TAlk and DIC fluxes from the Lower Changjiang to the ECS exhibited slight (insignificant) increases of 2–3% along the outflow way (Table 4).

### 3.4. Distributions of pH and Aragonite Saturation State in the Outer Changjiang Estuary

In March, $pH_T$ slightly increased from 7.90 to 8.14 in the outer estuary along with the salinity rise, while $\Omega_{arag}$ rose from 0.64 at the river mouth to 2.57 in the ECS offshore waters (Figures 5c and 5d). In the CDW area with a salinity range of 10–31, most March $pH_T$ were lower than 8.1, while March $\Omega_{arag}$ values were no more than 2.0. At the two northwest stations affected by YSCC during our March 2015 cruise, $pH_T$ and $\Omega_{arag}$ values were lower than other stations with similar salinity. Except for the northwest stations affected by YSCC, both $pH_T$ and $\Omega_{arag}$ in March were linearly correlated with salinity.

In July, distributions of $pH_T$ and $\Omega_{arag}$ were complex in the outer Changjiang estuary (Figures 5g and 5h). The surface-water $pH_T$ varied from 7.69 to 8.79, while the bottom-water $pH_T$ values were lower than 8.1. Most low-salinity $\Omega_{arag}$ ranged from 0.79 to 1.46, which was similar to the results obtained in March (i.e.,

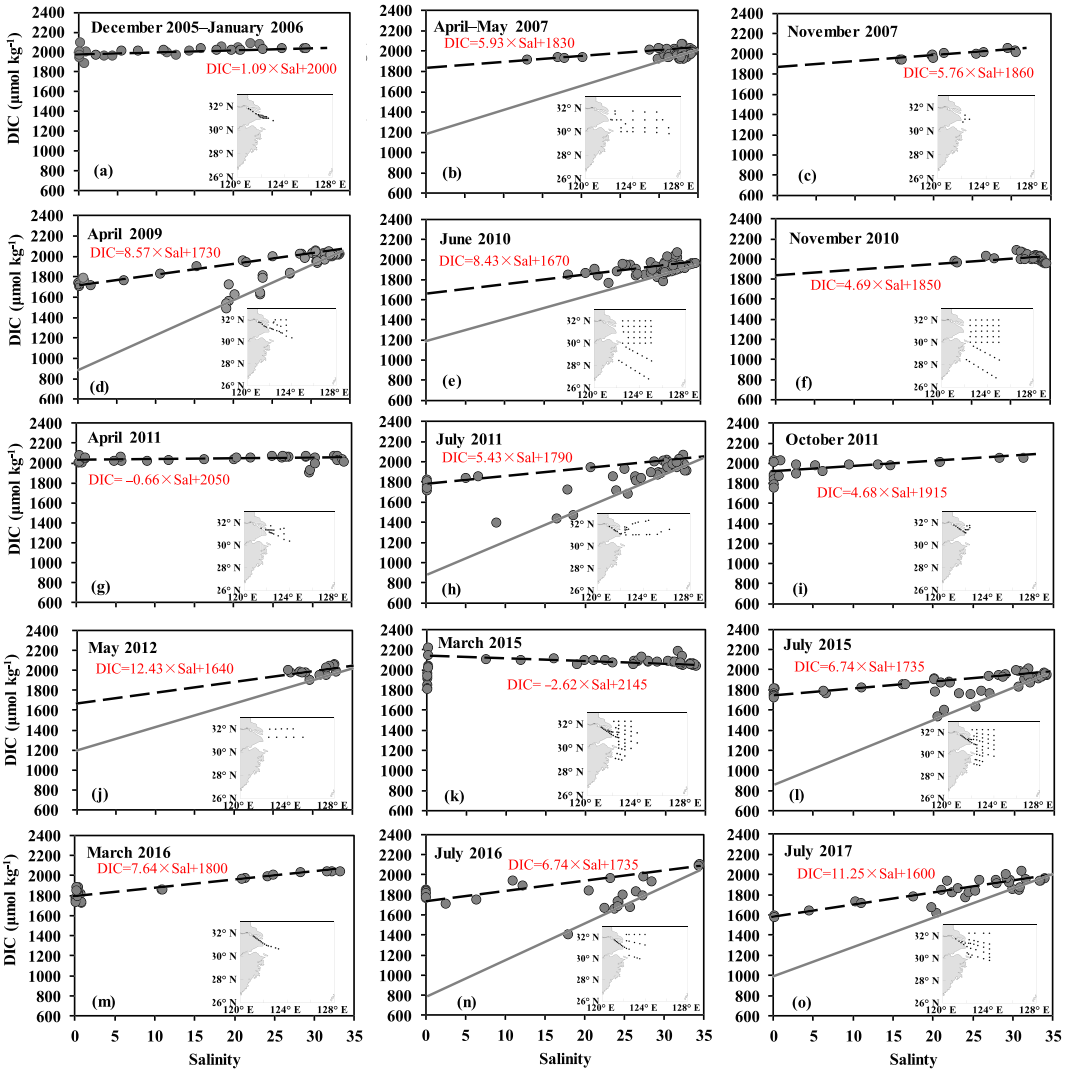


**Figure 7.** Sea surface dissolved inorganic carbon (DIC) versus salinity in the outer Changjiang Estuary during 2005–2017. Data in late 2005 and early 2006 are from Zhai et al. (2007), while data in 2007 are from Zhai and Hong (2012) and Zhai, Chen, et al. (2014). Data in May 2012 are from Zhai (2018), while data in 2015 have been partially published by Liu and Zhai (2016). Inserted panels show sampling sites. Broken lines together with equations are the assumed conservative mixing lines. Grey solid lines are plotted to determine effective concentrations considering the maximum DIC drawdown from biological production.

the low-salinity March $\Omega_{arag}$ values of 1.00–1.50 at the salinity of 10–20). Extremely high values of sea surface $pH_T$ (8.79) and $\Omega_{arag}$ (7.75) at salinity 18 were obtained at a southeastern station where we observed an algae bloom during the field survey. The high $pH_T$ values (from 7.78 to 8.55) and $\Omega_{arag}$ (from 1.59 to 6.15) were obtained in the high-salinity surface waters (salinity >20). In contrast, the bottom-water $pH_T$ (7.81–8.08) and $\Omega_{arag}$ values (1.39–2.82) were usually lower than their surface-water values in moderate and high salinity areas of the outer estuary.

## 4. Discussion

### 4.1. Long-Term Trend in TAlk and DIC Fluxes From the Changjiang River

Unlike the Mississippi with an increase in TAlk flux of ~70% over the twentieth century (Raymond et al., 2008), Changjiang TAlk transport flux varied around a nearly stable average over the past 55 years (Figure 8a). Similarly, water discharge from the Changjiang exhibited no long-term trend, even after the

**Table 4**
*Summary of Water Discharge (Q) Weighted Mean Concentrations (a) and Fluxes ($F = a \times Q$) Estimated in This Study*

| | $a_{TAlk}$ | $a_{DIC}$ | $F_{TAlk}$ | $F_{DIC}$ |
|---|---|---|---|---|
| | μmol/L | μmol/L | $10^{12}$ mol/year | $10^{12}$ mol/year |
| Datong Station (1963–1999) [a] | 1,763 ($n$=12, $R^2$=0.97) | 1,819 ($n$=12, $R^2$=0.97) | 1.58±0.21 | 1.63±0.22 |
| Datong Station (2015–2016) | 1,646 (n=14, $R^2$=0.96) | 1,670 (n=16, $R^2$=0.96) | 1.49–1.71 | 1.51–1.74 |
| Riverine flux estimation (West of Chongming Island, 2005–2017) | 1,673 (n=19, $R^2$=0.99) | 1,714 (n=18, $R^2$=0.99) | 1.44±0.20 | 1.48±0.21 |
| Export flux estimation (2005–2017) | 1,687 (n=15, $R^2$=0.98) | 1,721 (n=15, $R^2$=0.98) | 1.46±0.20 | 1.49±0.21 |

*Note*. Errors showed influences of standard deviations of Changjiang water discharge on the flux estimation.
[a]These data were based on results reported by Liu et al. (2002).

operation and maintenance of the Three Gorges Dam (Figure 8b). In the Changjiang Basin, intensive cultivation of crops and rice has been established for thousands of years, likely buffering the effect of potential chemical weathering enhancement from anthropogenic activities such as agricultural fertilization and sewage drainage (Guo, Wang, et al., 2015). According to Liu and Wang (2013), the Changjiang Basin experienced three agricultural development stages including extensive cultivation (~220 BCE–300 CE), intensive development of the plain (~300–1360 CE) and overdevelopment of the hilly regions (1370–1850 CE). Now it is in a stagnation stage due to the rapid industrialization and urbanization (Liu & Wang, 2013). By contrast, America has a relatively short history for about 200 years and its extensive agriculture is a relatively recent activity (He et al., 2015). The recent agricultural practices are changing American soil chemistry (Oh & Raymond, 2006; West & McBride, 2005) and thereby likely increasing the riverine TAlk transport flux.

The dissolved silicate (DSi), another major product of chemical weathering, also showed relatively stable concentration (100–150 μmol/L) and flux (~$7 \times 10^{10}$ mol/year) in the Lower Changjiang over the past several decades (Figures 8c and 8d). These data provide further evidence supporting the possible buffering effect of the Changjiang Basin on the potential chemical weathering enhancement from anthropogenic activities.

### 4.2. Effects of Riverine Carbonate Inputs on Nearshore pH and Aragonite Saturation State

To distinguish the complex coastal processes in the Changjiang Estuary, we quantitatively analyzed the ideal effects of DIC addition/removal (ΔDIC, relative to the baseline value along relevant conservative mixing line, with a positive value indicating the addition and a negative value indicating the removal) on [$CO_3^{2-}$], $pH_T$ and $\Omega_{arag}$ at different salinities (from 15 to 34) based on equations (2) and (4) at 25 °C (Figure 9). ΔDIC was defined as equation (14):

$$\Delta DIC = DIC - DIC^{conservative} \quad (14)$$

At a given salinity, [$CO_3^{2-}$], $pH_T$ and $\Omega_{arag}$ in the river plume waters decreased along with ΔDIC increase. In other words, net community production (respiration and/or remineralization) induced DIC removal (addition), raising (diminishing) [$CO_3^{2-}$], $pH_T$ and $\Omega_{arag}$. At a given ΔDIC, [$CO_3^{2-}$] and $\Omega_{arag}$ increased along with salinity increase. $pH_T$ was relatively insensitive to salinity change when ΔDIC ranged from −200 to 50 μmol/kg (Figure 9b). When ΔDIC > 50 μmol/kg, $pH_T$ increased along with salinity increase. When ΔDIC < −200 μmol/kg, however, $pH_T$ decreased along with salinity increase, which needs further investigation. Note that $\Omega_{arag}$ variations mostly depend on [$CO_3^{2-}$] during the dilution process, since the quotient of [$Ca^{2+}$] and $K^*_{sp\ arag}$ varies limitedly (<5%) at a salinity range from 15 to 32 (see Figure S6 related to Zhai et al., 2015).

Most field-data-based plots of [$CO_3^{2-}$], $pH_T$ and $\Omega_{arag}$ in July cruises followed the modeling results (Figure 9), suggesting that the modeling results were generally realistic. Excluding the metabolic processes (ΔDIC = 0), a decline in salinity of one unit led to a $pH_T$ decrease of 0.0053 and $\Omega_{arag}$ decline of 0.083 in the Changjiang Estuary. Based on Figures 9b and 9c, we reorganized new plots with ΔDIC versus salinity (Figure 10). The dashed lines in Figure 10 were critical isolines of $pH_T$ and $\Omega_{arag}$. These critical isolines were equivalent to the below partial differential equations:

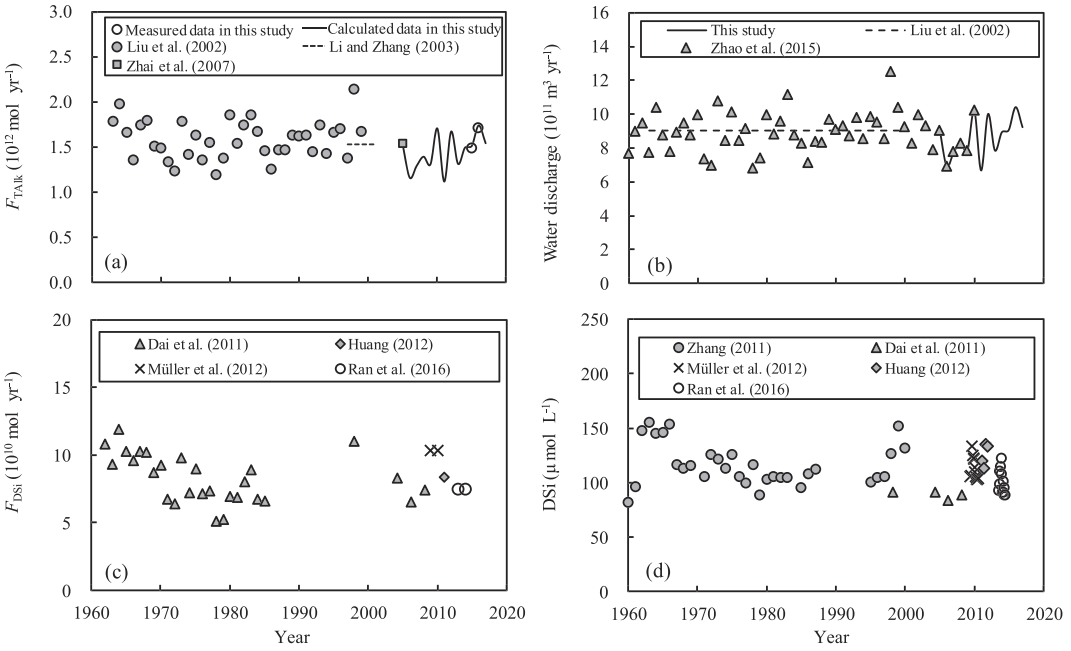


**Figure 8.** Time series of yearly fluxes of (a) total alkalinity, (b) freshwater, and (c) dissolved silicate in the Lower Changjiang from the 1960s to 2017. The 2005–2017 yearly fluxes of total alkalinity were calculated based on equation (10). Panel (d) shows the evolution of dissolved silicate concentrations in the lower Changjiang River during the past decades, synthesizing literature data from Dai et al. (2011), Zhang (2011), Huang (2012), Müller et al. (2012), and Ran et al. (2016).

$$\left[(\partial \mathrm{pH_T}/\partial \mathrm{Salinity})/(\partial \mathrm{pH_T}/\partial \mathrm{DIC})_{\mathrm{TAlk}}\right]_{\mathrm{pHT}\sim 7.9} = 3.23 \quad (15)$$

$$\left[(\partial \mathrm{pH_T}/\partial \mathrm{Salinity})/(\partial \mathrm{pH_T}/\partial \mathrm{DIC})_{\mathrm{TAlk}}\right]_{\mathrm{pHT}\sim 8.1} = 0.90 \quad (17)$$

$$\left[(\partial \Omega_{\mathrm{arag}}/\partial \mathrm{Salinity})/(\partial \Omega_{\mathrm{arag}}/\partial \mathrm{DIC})_{\mathrm{TAlk}}\right]_{\Omega\mathrm{arag}\sim 1.5} = 8.75 \quad (18)$$

$$\left[(\partial \Omega_{\mathrm{arag}}/\partial \mathrm{Salinity})/(\partial \Omega_{\mathrm{arag}}/\partial \mathrm{DIC})_{\mathrm{TAlk}}\right]_{\Omega\mathrm{arag}\sim 3.0} = 7.03 \quad (19)$$

When coastal $pH_T$ was close to a relatively low value of 7.9, the further $pH_T$ decrease under a salinity decline of one unit could be counteracted by a ΔDIC decrease of 3.23 μmol/kg. If the coastal $pH_T$ approached 8.1, it exhibited quite insensitive to salinity changes. The effect of a unit of salinity decrease on $\Omega_{arag}$ decline was expected to be counteracted by a ΔDIC decrease of 8.75 μmol/kg when coastal $\Omega_{arag}$ was close to a critical value of 1.5, while it was equivalent to a ΔDIC decrease of 7.03 μmol/kg when coastal $\Omega_{arag}$ was close to 3. This illustrates that high $pH_T$ and $\Omega_{arag}$ were relatively insensitive to salinity changes as compared with low $pH_T$ and $\Omega_{arag}$. Figure 10 also showed that, data-based plots of $pH_T$ and $\Omega_{arag}$ mostly located in the correct sections, suggesting that this model could be applied to predict coastal $pH_T$ and $\Omega_{arag}$ in the river plume area during the flood season.

In the outer Changjiang Estuary with salinity >10, the survey-based lowest $\Omega_{arag}$ values in bottom waters was detected at 1.52 in July 2016 and 1.39 in July 2017. Both were lower than the lowest value in July 2009 ($\Omega_{arag}$ ~1.7) reported by Chou et al. (2013). This is likely due to stronger respiration-induced bottom acidification induced by the increased amount of sinking organic matter produced in the surface water. The latter was evidenced by an increase in sea surface DO in wet seasons during the recent decade. The survey-based highest sea surface DO in 2009 was measured at ~400 μmol $O_2$/kg in spring (from late April to middle May) and ~300 μmol $O_2$/kg in summer (from late June to middle July) in the CDW area (Chou et al., 2013). During our summer cruises, however, the highest sea surface DO in the CDW reached 478 μmol $O_2$/kg in July 2015 (Figure 3h), indicating elevated biological production in the outer Changjiang Estuary. Although the coastal acidification caused by the river water input could be counteracted to some

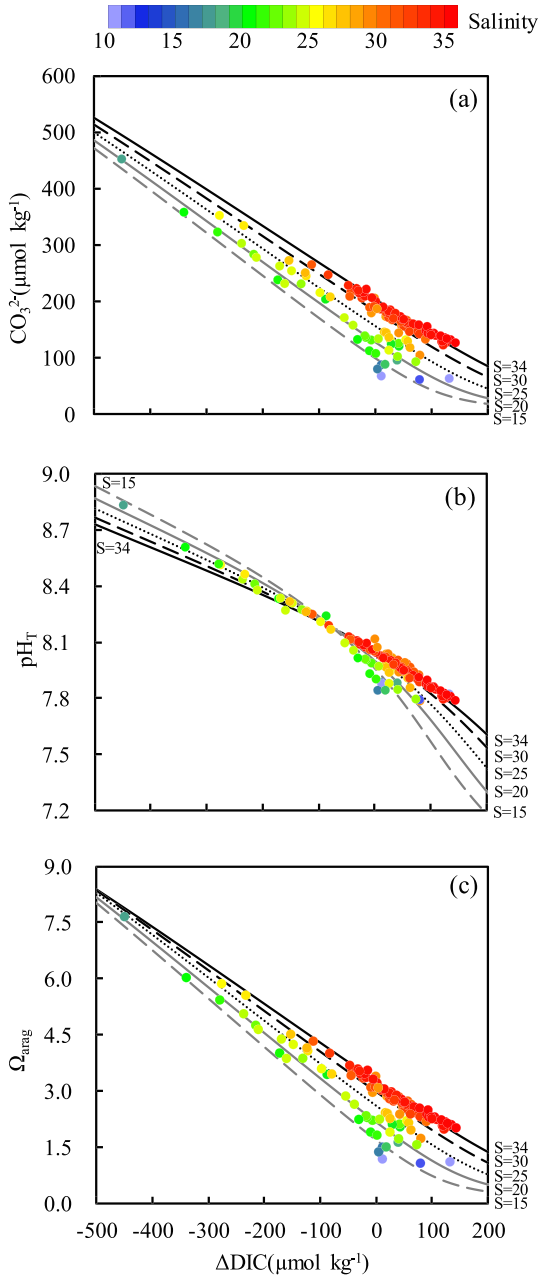


**Figure 9.** Modeled relationship of (a) $[CO_3^{2-}]$, (b) $pH_T$ and (c) $\Omega_{arag}$ versus ΔDIC at different salinity in the Changjiang Estuary (at 25 °C). ΔDIC refers to equation (14). Colored circles show real data with salinity obtained in our July surveys in 2015 and 2016.

extent by the high net primary production in surface waters (Chou et al., 2013), the net community respiration and/or remineralization of increasing sinking organic matters would produce more $CO_2$ and further the acidification in the subsurface waters. If subsurface DIC addition was more than 190 μmol/kg, the coastal $\Omega_{arag}$ would be lower than a critical value of 1.5 in the Changjiang Estuary (salinity <34) based on our model results, indicating that the local calcifying marine organisms would be under severe threat.

To further investigate the potential environmental impacts of terrestrial carbonate flux in different system, we plotted the similar diagram combining effects of water dilution and ΔDIC on coastal $\Omega_{arag}$ dynamics in the Mississippi river plume, incorporating our earlier results in the Yalu River plume (Zhai et al., 2015), and an ideal rainwater dilution case. These estuaries received different levels of terrestrial weathering products (Table S1 in the supporting information). Considering the rainwater dilution case, $[(\partial\Omega_{arag}/\partial Salinity)/(\partial\Omega_{arag}/\partial DIC)_{TAlk}]_{\Omega arag\ \sim 1.5}$ = 10.0 (Figure 11a), that is, the effect of a unit of salinity decrease on $\Omega_{arag}$ decline was expected to be counteracted by a ΔDIC decrease of 10 μmol/kg when $\Omega_{arag}$ was close to 1.5. Since this ideal case shared nearly the same seawater end-member with the Changjiang case (Figure 11a), the comparison between the two cases suggested that terrestrial carbonate inputs from Changjiang decreased the freshwater-dilution-induced suppression of coastal $\Omega_{arag}$ by 12% (10.0 versus 8.75). In the Yalu River plume area, $[(\partial\Omega_{arag}/\partial Salinity)/(\partial\Omega_{arag}/\partial DIC)_{TAlk}]_{\Omega arag\ \sim 1.5}$ = 6.73 (Figure 11a), consistent with our earlier result between 6.1 and 7.7 (Zhai et al., 2015). The freshwater end-member values of DIC and TAlk in the Yalu River estuary are only 320–800 μmol/kg (Zhai, Zheng, et al., 2014; Zhai et al., 2015), approximately 1,000 μmol/kg lower than those in the Changjiang Estuary. However, its seawater end-member is much different from the Changjiang river plume and rainwater dilution cases (Figure 11a). In the Mississippi river plume, $[(\partial\Omega_{arag}/\partial Salinity)/(\partial\Omega_{arag}/\partial DIC)_{TAlk}]_{\Omega arag\ \sim 1.5}$ = 9.43 (Figure 11a), suggesting that the buffering effect of its coastal carbonate system against the freshwater-dilution-induced $\Omega_{arag}$ suppression was between the Changjiang river plume and rainwater dilution cases.

Considering the chemical weathering source of riverine carbonate (Gaillardet et al., 1999), riverine $Ca^{2+}$ inputs should also affect estuarine/coastal $\Omega_{arag}$ dynamics. Although the riverine $Ca^{2+}$ inputs further increased the buffering effect of coastal carbonate system against the freshwater-dilution-induced $\Omega_{arag}$ suppression by 5–12% (Figure 11b), the combined effect of freshwater dilution and ΔDIC on estuarine/coastal $\Omega_{arag}$ dynamics showed similar results (Figure 11b) to the above-discussed pattern (Figure 11a).

### 4.3. Marine Alteration of Terrestrial Carbonate System Due to Biological DIC Drawdown in Wet Seasons

In the northwest ECS off the estuarine maximum turbidity zone, biological primary production is determined as high as 80–100 mmol C · m$^{-2}$ · day$^{-1}$ in spring and summer (Gong et al., 2003; Ning et al., 2004), leading to net removal of DIC in surface waters as compared with the conservative mixing lines obtained during our wet-season cruises (Figure 7). To evaluate the biological drawdown of DIC in the outer estuary in wet seasons from April to September, we calculated ΔDIC in relevant data sets (Figure 7) against the conservative water mixing lines, following equation (14). In those wet seasons during 2005–2017, survey-averaged ΔDIC ranged from −54 to −211 μmol/kg (Table 5), accompanied by oversaturated DO values

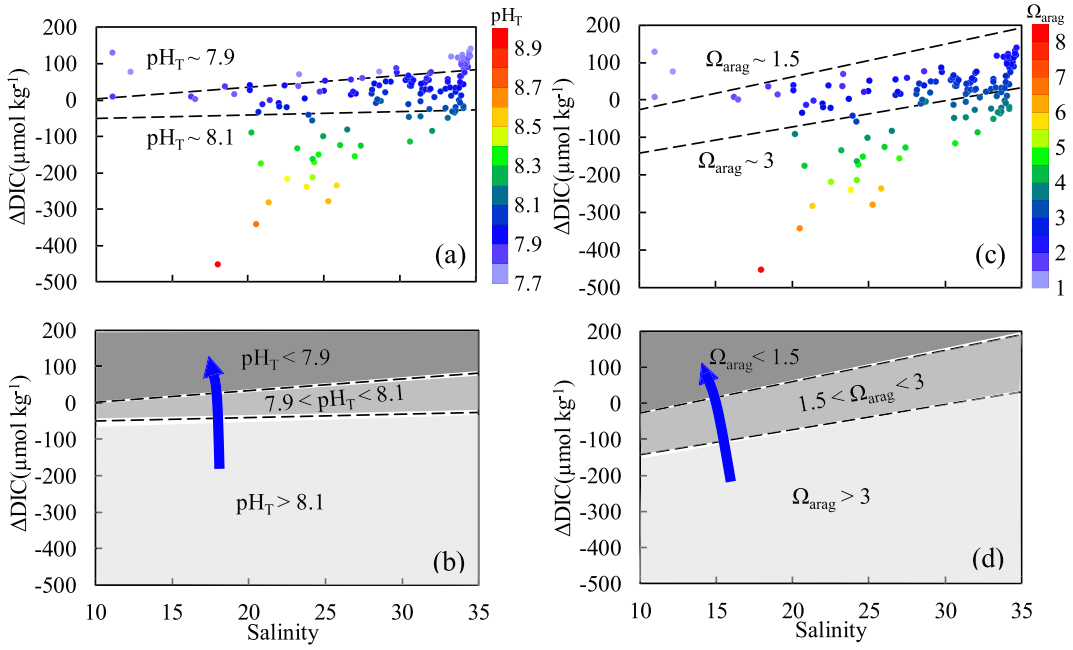


**Figure 10.** Combined effects of riverine water dilution and metabolic-process-induced DIC addition/removal (ΔDIC) on $pH_T$ (a–b) and $\Omega_{arag}$ (c–d) in the Changjiang Estuary in summer in 2015–2016 (at 25 °C). ΔDIC refers to equation (14). Based on conservative water mixing models in July 2015 (equations (2) and (3)), the estimated $pH_T$ ~7.9 line is ΔDIC (μmol/kg) = 3.23 × Salinity – 29.97, and the estimated $pH_T$ ~8.1 line is ΔDIC (μmol/kg) = 0.90 × Salinity – 58.55; the estimated $\Omega_{arag}$ ~1.5 line is ΔDIC (μmol/kg) = 8.75 × Salinity – 114.25, and the estimated $\Omega_{arag}$ ~3 line is ΔDIC (μmol/kg) = 7.03× Salinity – 213.10. Colored circles in panels (a) and (c) show real data with $pH_T$ and $\Omega_{arag}$ values obtained in our July surveys in 2015 and 2016. Blue arrows in panels (b) and (d) sketch the proportional relationship shown by equations (14)–(17).

(averaged 115–195%) and quite low DIC:TAlk ratios (averaged 0.81–0.89). To verify the ΔDIC calculation, we compared the ΔDIC with Excess DIC (the departure from air-equilibrated DIC, Zhai, 2018). Results showed that the two estimates were roughly comparable with each other (Table S2), suggesting that both of them measured the biological drawdown of DIC.

Together with the plume residence time (half a month, sustaining an algal bloom) and mixed layer depth (5–10 m), net community production (NCP) in the Changjiang Estuary during wet seasons were estimated at 28–107 mmol C · $m^{-2}$ · $day^{-1}$ (Table 5). Our estimates were close to the depth-integrated primary production obtained in the inner shelf of the ECS, such as 30–80 mmol C · $m^{-2}$ · $day^{-1}$ measured in March and June 1998 (Gong et al., 2003) and 40–100 mmol C · $m^{-2}$ · $day^{-1}$ measured in June, July and August of 2003–2005 (Chen et al., 2009). The summertime NCP values in this study were also comparable to those obtained in the same area in July 1986 (~125 mmol C · $m^{-2}$ · $day^{-1}$) by Ning et al. (1988) and in August 2009 (~150 mmol C · $m^{-2}$ · $day^{-1}$) by Wang et al. (2017). Based on the NCP value (averaged 54 mmol C · $m^{-2}$ · $day^{-1}$), yearly bloom duration time (25–50% of the wet season, 1.5–3 months), and the bloom occurrence area (10–15% of the ECS area in spring and summer; He et al., 2013; Guo, Zhai, et al., 2015), we estimated the biological DIC removals off the Changjiang Estuary at (1.13–3.38) × $10^{11}$ mol C/year. The NCP induced DIC removals should be balanced by all those exogenous DIC sources, including riverine inputs and the atmospheric $CO_2$ intrusion. Therefore, the NCP evaluation suggested that at most 11–34% of the DIC flux discharged from the Changjiang River in wet seasons could be sequestered in nearshore areas by biological production.

To further evaluate the effect of offshore biological drawdown of DIC on flux estimation, we rewrote Officer (1979) equation for biological-induced flux loss ($L_{\_bio}$) in the estuary as $L_{\_bio} = Q \times (C_0 - C_0^*{}_{\_bio}) \times \Gamma$, where $Q$ was water discharge, $C_0$ was DIC concentration at river end-member (Table 2), $C_0^*{}_{\_bio}$ was the specific effective DIC concentration at zero salinity considering the maximum removal (Table 3), $\Gamma$ indicated the proportion of community-production-dominated stations against all stations during the field surveys (0.40 in April–May 2007, 0.27 in April 2009, 0.39 in June 2010, 0.21 in July 2011, 0.40 in May 2012, 0.17 in July

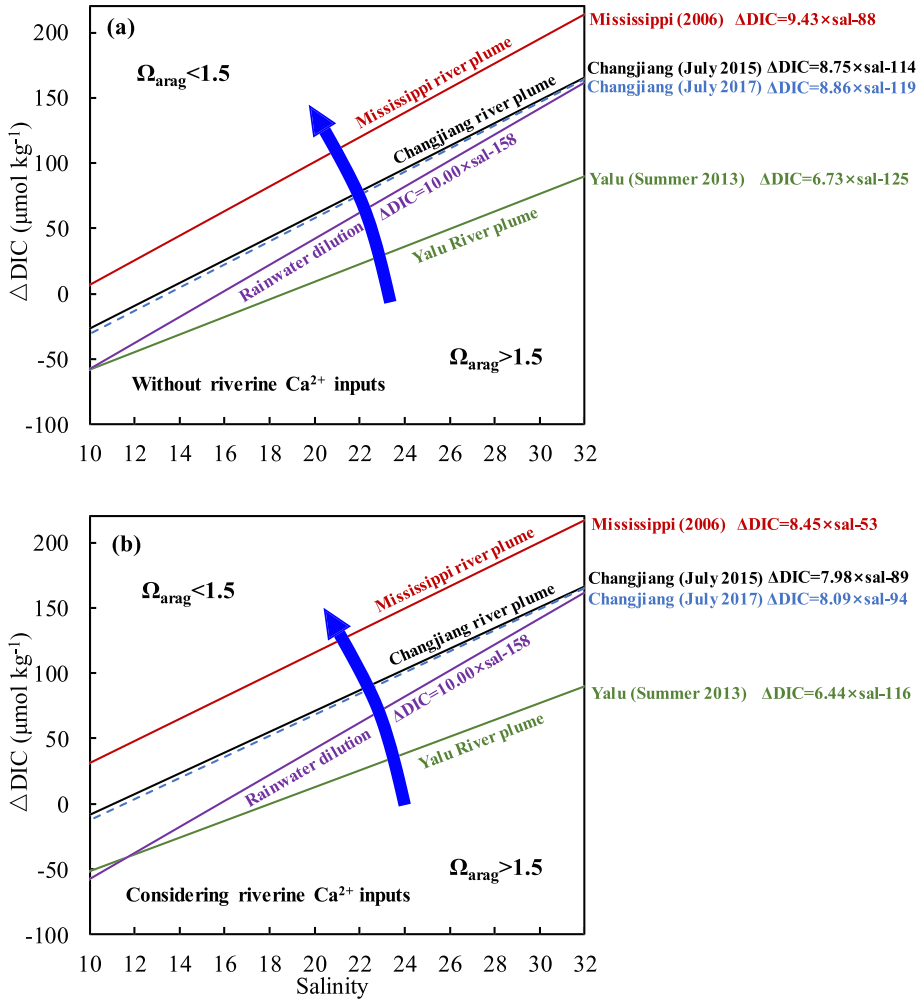


**Figure 11.** Diagrams sketching combined effects of freshwater dilution (Salinity ranging 10–32) and DIC addition/removal (ΔDIC) on $\Omega_{arag}$ (at 25 °C) in Changjiang, Mississippi and Yalu River plumes. The rainwater dilution case is also plotted as a reference. ΔDIC refers to equation (14). Colored lines show critical lines of $\Omega_{arag}$~1.5 in different regimes. Relevant conservative water mixing models refer to Supplementary Table S1. Briefly, the Mississippi has a relatively high level of riverine bicarbonate alkalinity of 2450±500 μmol/kg in the flood season (Hu et al., 2017). The river end-member for DIC was assumed 30 μmol/kg higher than that for TAlk (Guo et al., 2012). The seawater end-member values of carbonate system in the Gulf of Mexico were averaged from three 2006 cruises (Guo et al., 2012). A two-end-member water mixing model was assumed in the Mississippi river plume in its flood seasons (Cai, 2003). The Changjiang river plume cases refer to equations (2)–(5) and (18). The rainwater dilution case is based on the typical and air-equilibrated Kuroshio carbonate system (Bai et al., 2015). The Yalu River plume case refers to Zhai et al. (2015). The blue arrow sketches the proportional relationship between partial differential effects of salinity change and ΔDIC, either from metabolic processes or from the anthropogenic $CO_2$ invasion. Panel (b) considered riverine $Ca^{2+}$ inputs at a half of corresponding riverine TAlk values. It is worthwhile to note that the river end member of $Ca^{2+}$ in the Changjiang Estuary was measured at 954 ±54 μmol/kg by Qi (2013) during our April, July, and October 2011, and February 2012 surveys, slightly higher than a half of the Lower Changjiang TAlk values (Tables 1, 2).

2015, 0.36 in July 2016, and 0.27 in July 2017). Therefore, the biologically induced DIC flux loss in the outer estuary was estimated at (4.31–22.97) × $10^3$ mol/s (Table 3). In wet seasons, 9–20% (averaged at 12.1 ± 3.5%) of the estuarine DIC export flux from the Changjiang was sequestered in the coastal zone (Figure 7), while TAlk export flux was rarely affected (Figure 6). The biological DIC removals derived from the effective concentration method was comparable to that from the NCP estimation.

This biological alteration clearly contributed to the formation of relatively low DIC:TAlk ratio in offshore waters (<0.9 versus typically >1.0 at the river end; Figures 12 and 13). Although the riverine carbonate system in a limited region can be diluted by offshore waters (Figure 12), the dilution effect did not really

**Table 5**
*Data Summary (Mean ± SD) of Our Springtime and Summertime surveys, Including Sea Surface Salinity, Temperature, Dissolved Oxygen (DO), DIC:TAlk Ratio, DIC Addition/Removal (ΔDIC, Refers to Figure S6 for Details), and Net Community Production (NCP) Estimated in the Changjiang River Plume*

| Survey | Salinity | Temperature (°C) | DO saturation (%) | DIC:TAlk ratio | ΔDIC (μmol/kg) | NCP (mmol C · $m^{-2}$ · $day^{-1}$) |
|---|---|---|---|---|---|---|
| April–May 2007 | 32.7±1.1 | 16.7±1.1 | 115±10 | 0.86±0.01 | −68±23 | 35±12 |
| April 2009 | 28.9±4.7 | 14.3±0.8 | 133±35 | 0.85±0.05 | −121±115 | 62±59 |
| June 2010 | 30.5±2.2 | 21.9±1.3 | 112±11 | 0.85±0.01 | −54±31 | 28±16 |
| July 2011 | 26.2±6.0 | 25.4±2.1 | 195±37 | 0.84±0.05 | −155±140 | 79±71 |
| May 2012 | 31.1±1.8 | 14.4±0.9 | 113±7 | 0.89±0.02 | −57±35 | 30±18 |
| July 2015 | 29.1±5.0 | 25.2±1.4 | 134±31 | 0.84±0.03 | −102±97 | 52±50 |
| July 2016 | 23.9±2.6 | 26.1±1.0 | 138±29 | 0.81±0.05 | −211±102 | 107±51 |
| July–August 2017 | 24.6±4.7 | 28.3±2.0 | 132±21 | 0.85±0.03 | −74±60 | 38±31 |

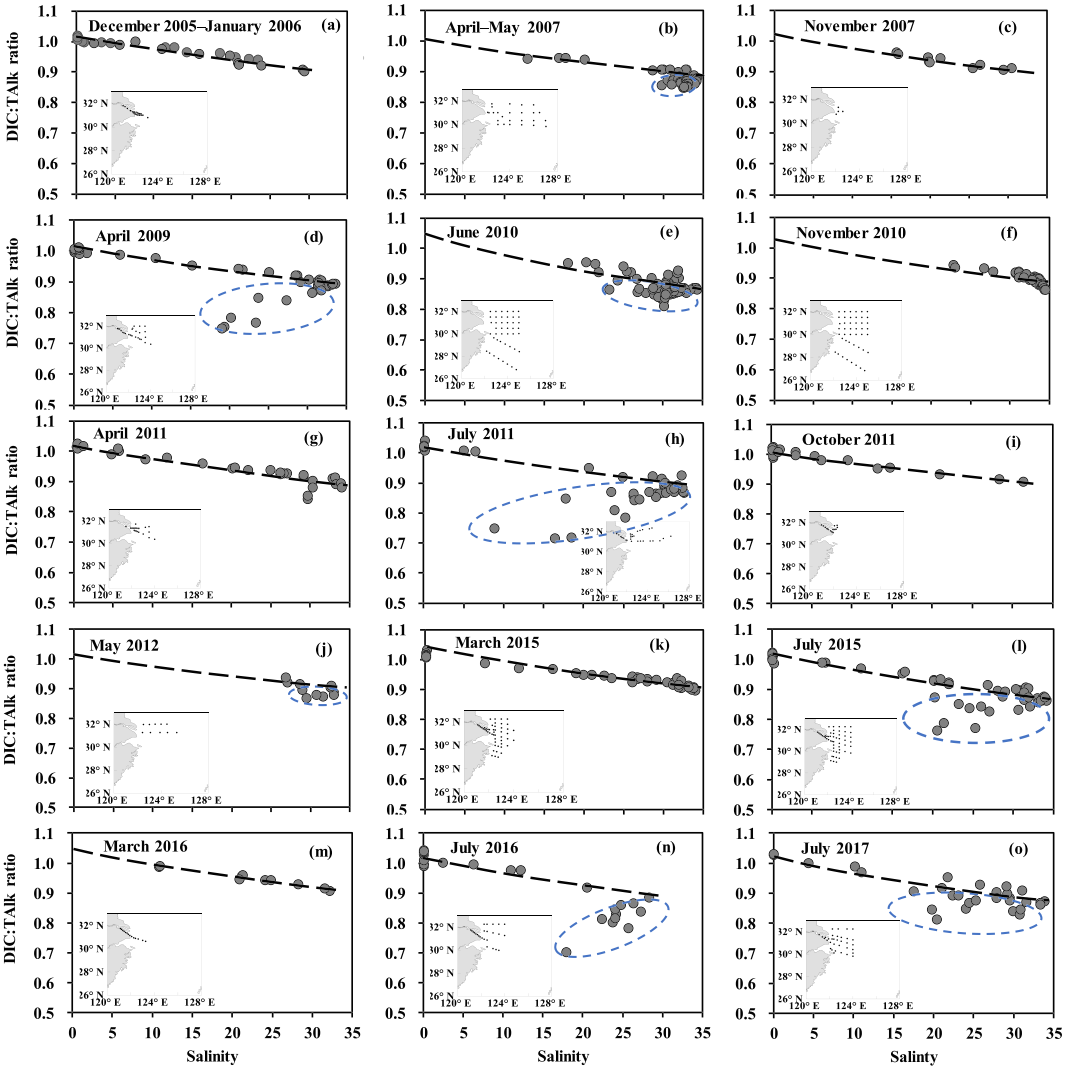


**Figure 12.** Sea surface DIC:TAlk ratio versus salinity in the outer Changjiang Estuary. Data in late 2005 and early 2006 are from Zhai et al. (2007), while data in 2007 are from Zhai and Hong (2012) and Zhai, Chen, et al. (2014). Data in May 2012 are from Zhai (2018), while data in 2015 have been partially published by Liu and Zhai (2016). Inserted panels show relevant sampling sites. Broken curves are the assumed conservative water mixing lines, combining the conservative water mixing lines of TAlk and DIC from Figures 7 and 8. Dashed ellipses circle those data points showing biological drawdown of DIC.

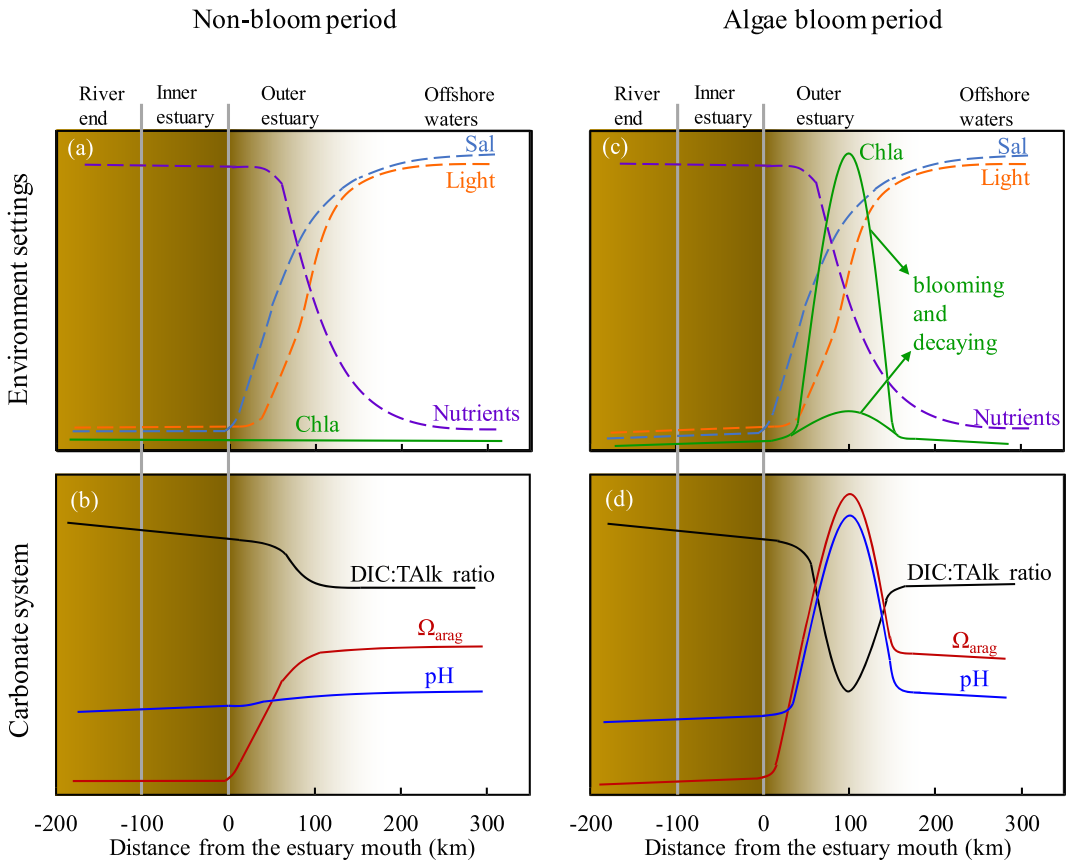


**Figure 13.** Diagrams sketching changes in environmental settings and those indicative carbonate system parameters along the flow-path from the estuary to the sea, during (a and b) nonbloom periods and (c and d) algae bloom periods. The colored background shows turbidity variations from river-end to the offshore area and the darker brown indicates the turbidity maximum zone around the river mouth.

transform terrestrial carbonate system to oceanic carbonate system. This is because oceanic $CO_3^{2-}$ ions will be titrated by terrestrial free $CO_2$ that was discharged from the rivers (i.e., $CO_2 + CO_3^{2-} + H_2O \rightarrow 2HCO_3^-$), during which neither DIC nor TAlk changes, and the DIC:TAlk ratio will be averaged. In a long-term run, the typical seawater DIC:TAlk ratio of <0.9 must be maintained by the biological alteration (removing free $CO_2$ from seawater but without a loss of $CO_3^{2-}$, during which DIC declines but TAlk remains unchanged, and the DIC:TAlk ratio decreases). Our findings support Redfield et al. (1963) earlier argument on "the influence of organisms on the composition of seawater".

According to Chen et al. (2014), the summertime $CO_2$ sink in the CDW has increased since the 2000s. In the 1990s, the lowest springtime and/or summertime sea surface $pCO_2$ was recorded off Changjiang Estuary at ~200 μatm (Peng et al., 1999; Tsunogai et al., 1999; Wang et al., 2000; Zhang et al., 1997; Zhang et al., 1999). In the early 2000s, quite low $pCO_2$ of 110–140 μatm was detected in this region (Chen et al., 2006; Tan et al., 2004; Tseng et al., 2014). In the recent decade, however, extremely low sea surface $pCO_2$ values of 30–80 μatm were frequently observed in the CDW area (Figure S7), which was only 10–20% of the air-equilibrated level. This trend is consistent with the substantial increases in riverine dissolved inorganic nitrogen (approximately tenfold) and dissolved inorganic phosphate (approximately sixfold) deliveries (Dai et al., 2011; Liu et al., 2002) and the corresponding algal blooms (Wang & Wu, 2009; Zhou et al., 2008) over the past several decades. The CDW biological production may exert potentially larger impacts on the coastal carbonate chemistry dynamics than before, especially in wet seasons.

Globally, the marine alteration of terrestrial carbonate system by biological production exists in many large river plume areas (Chen et al., 2012), such as the Amazon plume (Cooley et al., 2007; Cooley & Yager, 2006; Lefèvre et al., 2017; Körtzinger, 2003; Ternon et al., 2000), the Mississippi plume (Cai, 2003; Guo et al., 2012),

and the Pearl River plume, China (Cao et al., 2011; Dai et al., 2008). The wet-season NCP values observed in some large-river plume waters were 36 mmol C · $m^{-2}$ · $day^{-1}$ in the Pearl River plume in summer 2008 (Cao et al., 2011), 100–133 mmol C · $m^{-2}$ · $day^{-1}$ in the Amazon plume in May 1996 (Ternon et al., 2000), and ~90 mmol C · $m^{-2}$ · $day^{-1}$ in the Mississippi plume in June 2006 (even ~300 mmol C · $m^{-2}$ · $day^{-1}$ in August 2004; Guo et al., 2012). In these river-estuary-coastal continuums, biological productivity fronts may appear in appropriate plume areas with optimal light availability and nutrient utilization (Dagg et al., 2004; Ning et al., 1988, 2004; Figure S8), as sketched in Figure 13c. In the biological productivity fronts, the biological drawdown of DIC induces a substantial decline in DIC:TAlk ratio from >1 at the river end to as low as ~0.7 (Figure 12), and then it is mixed with offshore waters usually having a DIC:TAlk ratio of 0.8–0.9 (Figure 13d). The local decline in DIC:TAlk ratio is definitely accompanied by high pH and $\Omega_{arag}$ values in the river plume area (Figures 5g and 5h), as sketched in Figure 13d. This study provided a regional case quantifying the biological altering effect of the terrestrial carbonate system by biological production, which played the key role in transforming terrestrial carbonate system into seawater carbonate system. Given the fact that chemical buffering capacity slows down the air-sea equilibration of $CO_2$, the biological DIC drawdown in a bloom event has durative effects on the sea surface carbonate system for at least several weeks (Zhai, Chen, et al., 2014).

Apart from the biological production of organic matter, $CaCO_3$ dissolution also transformed free $CO_2$ to bicarbonate ion in several coastal zones without losses of seawater $CO_3^{2-}$ (e.g., Abril et al., 2003; Zhai et al., 2017), effectively lowering the aquatic DIC:TAlk ratio. This process may sequester the regenerated free $CO_2$ in subsurface waters where biogenic organic matter is respired (Chen, 1978). However, this issue needs further investigation in the future.

## 5. Conclusion

The Changjiang (Yangtze River) transported a large amount of carbonate into its estuary and the adjacent ECS, varying slightly from the historical long-term mean fluxes of $(1.58 \pm 0.21) \times 10^{12}$ mol TAlk/year and $(1.63 \pm 0.22) \times 10^{12}$ mol DIC/year during 1963–1999 (Liu et al., 2002) to the recently decadal mean fluxes of $(1.44 \pm 0.20) \times 10^{12}$ mol TAlk/year and $(1.48 \pm 0.21) \times 10^{12}$ mol DIC/year during 2005–2017. In comparison with a rainwater dilution case, the terrestrial carbonate inputs from Changjiang decreased the freshwater-dilution-induced suppression of coastal aragonite saturation state by 12%. In wet seasons, 9–20% of the estuarine DIC export fluxes from the Changjiang River were sequestered in nearshore areas by biological activities, while the TAlk fluxes were rarely affected. This process effectively altered the carbonate system from terrestrial feature (with DIC:TAlk ratios of >1.0) to the usual seawater feature (with DIC:TAlk ratios of <0.9).

Despite a regional study, our results support Alfred C. Redfield's argument on "the influence of organisms on the composition of seawater" in the 1960s or earlier. Moreover, the nearly stable average of Changjiang carbonate flux over the past 55 years is much different from the American case of century-long TAlk increase in some rivers, suggesting that the response of watershed chemical weathering to climate change and human activity varies in different systems, presumably relying on the land-use history and other physical and biogeochemical conditions. In the context of future atmospheric $CO_2$ rise and global warming (potentially enhancing chemical weathering in most watersheds), much remains to be investigated to quantitatively evaluate corresponding changes in riverine exports of those watershed chemical weathering products (such as carbonate and silicate) on a global scale.

**Acknowledgments**
AcknowledgementsThis research was jointly supported by the Oceanic Public Science and Technology Research Funds Projects of China (201505003), the National Natural Science Foundation of China (grants 91751207, 41276061, 41076044, and 40876040), and the National Basic Research Program of China (2009CB421204). Some sampling surveys were supported by the National Natural Science Foundation of China via Open Shiptime projects in the Changjiang Estuary (in 2015–2017, onboard *R/V* Runjiang 1) and in the East China Sea (in 2010, onboard *R/V* Kexue 3). The offshore samples in July 2011 were collected by Wei Qian onboard *R/V* Dongfanghong 2. Data collections were partially supported by the Visiting Fellowship (to Wei-dong Zhai) in the State Key Laboratory of Marine Environmental Science (Xiamen University). We also appreciate constructive comments and suggestions from two anonymous reviewers, which have improved the quality of this paper. The monthly water discharge data and mapping dataset of DO and carbonate system parameters reported in this study are available at figshare.com via https://doi.org/10.6084/m9.figshare.9932444 and https://doi.org/10.6084/m9.figshare.9768215, respectively. The other time series data directly used in this work are presented in the figures and tables, while yearly data showing variations in long-term run are also available at figshare.com via https://doi.org/10.6084/m9.figshare.9948308. Competing financial interests: The authors declare no competing financial interests.

## References

Abril, G., Etcheber, H., Delille, B., Frankignoulle, M., & Borges, A. V. (2003). Carbonate dissolution in the turbid and eutrophic Loire estuary. *Marine Ecology Progress Series*, *259*, 129–138. https://doi.org/10.3354/meps259129

Aufdenkampe, A. K., Mayorga, E., Raymond, P. A., Melack, J. M., Doney, S. C., Alin, S. R., et al. (2011). Riverine coupling of biogeochemical cycles between land, oceans, and atmosphere. *Frontiers in Ecology and the Environment*, *9*(1), 53–60. https://doi.org/10.1890/100014

Bai, Y., He, X.-Q., Pan, D.-L., Chen, C.-T. A., Kang, Y., Chen, X.-Y., & Cai, W.-J. (2014). Summertime Changjiang River plume variation during 1998–2010. *Journal of Geophysical Research: Oceans*, *119*, 6238–6257. https://doi.org/10.1002/2014JC009866

Bai, Y., Huang, T.-H., He, X.-Q., Wang, S.-L., Hsin, Y.-C., Wu, C.-R., et al. (2015). Intrusion of the Pearl River plume into the main channel of the Taiwan Strait in summer. *Journal of Sea Research*, *95*, 1–15. https://doi.org/10.1016/j.seares.2014.10.003

Bauer, J. E., Cai, W.-J., Raymond, P. A., Bianchi, T. S., Hopkinson, C. S., & Regnier, P. A. G. (2013). The changing carbon cycle of the coastal ocean. *Nature*, *504*(7478), 61–70. https://doi.org/10.1038/nature12857

Benson, B. B., & Krause, D. (1984). The concentration and isotopic fractionation of oxygen dissolved in fresh water and seawater in equilibrium with the atmosphere. *Limnology and Oceanography*, *29*, 620–632. https://doi.org/10.4319/lo.1984.29.3.0620

Boyle, E., Collier, R., Dengler, A. T., Edmond, J. M., Ng, A. C., & Stallard, R. F. (1974). On the chemical mass-balance in estuaries. *Geochimica et Cosmochimica Acta*, *38*, 1719–1728. https://doi.org/10.1016/0016-7037(74)90188-4

Cai, W.-J. (2003). Riverine inorganic carbon flux and rate of biological uptake in the Mississippi River plume. *Geophysical Research Letters*, *30*(2), 1032. https://doi.org/10.1029/2002GL016312

Cai, W.-J., Dai, M.-H., Wang, Y.-C., Zhai, W.-D., Huang, T., Chen, S.-T., et al. (2004). The biogeochemistry of inorganic carbon and nutrients in the Pearl River estuary and the adjacent Northern South China Sea. *Continental Shelf Research*, *24*, 1301–1319. https://doi.org/10.1016/j.csr.2004.04.005

Cai, W.-J., Guo, X.-H., Chen, C.-T. A., Dai, M.-H., Zhang, L.-J., Zhai, W.-D., et al. (2008). A comparative overview of weathering intensity and $HCO_3^-$ flux in the world's major rivers with emphasis on the Changjiang, Huanghe, Zhujiang (Pearl) and Mississippi Rivers. *Continental Shelf Research*, *28*, 1538–1549. https://doi.org/10.1016/j.csr.2007.10.014

Cai, W.-J., Hu, X.-P., Huang, W.-J., Murrell, M. C., Lehrter, J. C., Lohrenz, S. E., et al. (2011). Acidification of subsurface coastal waters enhanced by eutrophication. *Nature Geoscience*, *4*, 766–770. https://doi.org/10.1038/ngeo1297

Cai, W.-J., & Wang, Y.-C. (1998). The chemistry, fluxes and sources of carbon dioxide in the estuarine waters of the Satilla and Altamaha Rivers, Georgia. *Limnology and Oceanography*, *43*, 657–668. https://doi.org/10.4319/lo.1998.43.4.0657

Caldeira, K., & Wickett, M. E. (2003). Anthropogenic carbon and ocean pH. *Nature*, *425*(6956), 365–365. https://doi.org/10.1038/425365a

Cao, Z.-M., Dai, M.-H., Zheng, N., Wang, D.-L., Li, Q., Zhai, W.-D., et al. (2011). Dynamics of the carbonate system in a large continental shelf system under the influence of both a river plume and coastal upwelling. *Journal of Geophysical Research*, *116*, G02010. https://doi.org/10.1029/2010JG001596

Chen, C., Zhu, J., Beardsley, R. C., & Franks, P. J. S. (2003). Physical-biological sources for dense algal blooms near the Changjiang River. *Geophysical Research Letters*, *30*(10), 1515. https://doi.org/10.1029/2002GL016391

Chen, C.-C., Chiang, K.-P., Gong, G.-C., Shiah, F.-K., Tseng, C.-M., & Liu, K.-K. (2006). Importance of planktonic community respiration on the carbon balance of the East China Sea in summer. *Global Biogeochemical Cycles*, *20*, GB4001. https://doi.org/10.1029/2005GB002647

Chen, C.-C., Shiah, F.-K., Chiang, K.-P., Gong, G.-C., & Kemp, W. M. (2009). Effects of the Changjiang (Yangtze) River discharge on planktonic community respiration in the East China Sea. *Journal of Geophysical Research*, *114*, C03005. https://doi.org/10.1029/2008JC004891

Chen, C.-T. A. (1978). Decomposition of calcium carbonate and organic carbon in the deep oceans. *Science*, *201*(4357), 735–736. https://doi.org/10.1126/science.201.4357.735

Chen, C.-T. A. (2009). Chemical and physical fronts in the Bohai, Yellow and East China seas. *Journal of Marine Systems*, *78*, 394–410. https://doi.org/10.1016/j.jmarsys.2008.11.016

Chen, C.-T. A., Huang, T.-H., Fu, Y.-H., Bai, Y., & He, X.-Q. (2012). Strong sources of $CO_2$ in upper estuaries become sinks of $CO_2$ in large river plumes. *Current Opinion in Environmental Sustainability*, *4*, 179–185. https://doi.org/10.1016/j.cosust.2012.02.003

Chen, C.-T. A., Ruo, R., Pai, S.-C., Liu, C.-T., & Wong, G. T. F. (1995). Exchange of water masses between the East China Sea and the Kuroshio off northeastern Taiwan. *Continental Shelf Research*, *15*, 19–39. https://doi.org/10.1016/0278-4343(93)E0001-O

Chen, C.-T. A., & Wang, S.-L. (1999). Carbon, alkalinity and nutrient budget on the East China Sea continental shelf. *Journal of Geophysical Research*, *104*(C9), 20,675–20,686. https://doi.org/10.1029/1999JC900055

Chen, C.-T. A., Zhai, W.-D., & Dai, M.-H. (2008). Riverine input and air–sea $CO_2$ exchanges near the Changjiang (Yangtze River) Estuary: status quo and implication on possible future changes in metabolic status. *Continental Shelf Research*, *28*, 1476–1482. https://doi.org/10.1016/j.csr.2007.10.013

Chen, J.-S., Wang, F.-Y., Xia, X.-H., & Zhang, L.-T. (2002). Major element chemistry of the Changjiang (Yangtze River). *Chemical Geology*, *187*, 231–255. https://doi.org/10.1016/S0009-2541(02)00032-3

Chen, X., Song, J.-M., Yuan, H.-M., Li, X.-G., Li, N., Duan, L.-Q., & Qu, B.-X. (2014). $CO_2$ fluxes across the air-sea interface of the East China Sea in summer 2011 and the change tendency of regional carbon sink strength (in Chinese). *Acta Oceanologica Sinica*, *36*(12), 18–31. http://www.hyxb.org.cn/aos/ch/reader/view_abstract.aspx?flag=1&file_no=20141202

Chen, Z.-Y., Li, J.-F., Shen, H.-T., & Wang, Z.-H. (2001). Yangtze River of China: historical analysis of discharge variability and sediment flux. *Geomorphology*, *41*, 77–91. https://doi.org/10.1016/S0169-555X(01)00106-4

Chou, W.-C., Gong, G.-C., Hung, C.-C., & Wu, Y.-H. (2013). Carbonate mineral saturation states in the East China Sea: present conditions and future scenarios. *Biogeosciences*, *10*, 6453–6467. https://doi.org/10.5194/bg-10-6453-2013

Cooley, S. R., Coles, V. J., Subramaniam, A., & Yager, P. L. (2007). Seasonal variations in the Amazon plume-related atmospheric carbon sink. *Global Biogeochemical Cycles*, *21*, GB3014. https://doi.org/10.1029/2006GB002831

Cooley, S. R., & Yager, P. L. (2006). Physical and biological contributions to the western tropical North Atlantic Ocean carbon sink formed by the Amazon River plume. *Journal of Geophysical Research*, *111*, C08018. https://doi.org/10.1029/2005JC002954

Dagg, M., Benner, R., Lohrenz, S., & Lawrence, D. (2004). Transformation of dissolved and particulate materials on continental shelves influenced by large rivers: plume processes. *Continental Shelf Research*, *24*, 833–858. https://doi.org/10.1016/j.csr.2004.02.003

Dagg, M. J., Bianchi, T. S., Breed, G. A., Cai, W.-J., Duan, S., Liu, H., et al. (2005). Biogeochemical characteristics of the lower Mississippi River, USA, during June 2003. *Estuaries*, *28*(5), 664–674. https://doi.org/10.1007/BF02732905

Dai, A.-G., & Trenberth, K. E. (2002). Estimates of freshwater discharge from continents: latitudinal and seasonal variations. *Journal of Hydrometeorology*, *3*, 666–687. https://doi.org/10.1175/1525-7541(2002)003%3C0660:EOFDFC%3E2.0.CO;2

Dai, M.-H., Zhai, W.-D., Cai, W.-J., Callahan, J., Huang, B.-Q., Shang, S.-L., et al. (2008). Effects of an estuarine plume-associated bloom on the carbonate system in the lower reaches of the Pearl River estuary and the coastal zone of the northern South China Sea. *Continental Shelf Research*, *28*, 1416–1423. https://doi.org/10.1016/j.csr.2007.04.018

Dai, Z.-J., Du, J.-Z., Zhang, X.-L., Su, N., & Li, J.-F. (2011). Variation of riverine material loads and environmental consequences on the Changjiang (Yangtze) Estuary in recent decades (1955–2008). *Environmental Science & Technology*, *45*(1), 223–227. https://doi.org/10.1021/es103026a

Dickson, A. G. (1990). Standard potential of the reaction: AgCl(s) + 1/2$H_2$(g) = Ag(s) + HCl (aq), and the standard acidity constant of the ion $HSO_4^-$ in synthetic sea water from 273.15 to 318.15 K. *The Journal of Chemical Thermodynamics*, *22*, 113–127. https://doi.org/10.1016/0021-9614(90)90074-Z

Dickson, A. G. (1992). The development of the alkalinity concept in marine chemistry. *Marine Chemistry*, *40*, 49–63. https://doi.org/10.1016/0304-4203(92)90047-E

Dickson, A. G., Sabine, C. L., & Christian, J. R. (2007). Guide to best practices for ocean $CO_2$ measurements PICES Special Publication 3 (pp. 1–191). http://cdiac.ornl.gov/oceans/Handbook_2007.html

Doney, S. C., Fabry, V. J., Feely, R. A., & Kleypas, J. A. (2009). Ocean acidification: the other $CO_2$ problem. *Annual Review of Marine Science*, *1*, 169–192. https://doi.org/10.1146/annurev.marine.010908.163834

Ekstrom, J. A., Suatoni, L., Cooley, S. R., Pendleton, L. H., Waldbusser, G. G., Cinner, J. E., et al. (2015). Vulnerability and adaptation of US shellfisheries to ocean acidification. *Nature Climate Change*, *5*, 207–214. https://doi.org/10.1038/nclimate2508

Friis, K., Körtzinger, A., & Wallace, D. W. R. (2003). The salinity normalization of marine inorganic carbon chemistry data. *Geophysical Research Letters*, *30*(2), 1085. https://doi.org/10.1029/2002GL015898

Fry, C. H., Tyrrell, T., Hain, M. P., Bates, N. R., & Achterberg, E. P. (2015). Analysis of global surface ocean alkalinity to determine controlling processes. *Marine Chemistry*, *174*, 46–57. https://doi.org/10.1016/j.marchem.2015.05.003

Gaillardet, J., Dupré, B., Louvat, P., & Allègre, C. J. (1999). Global silicate weathering and $CO_2$ consumption rates deduced from the chemistry of large rivers. *Chemical Geology*, *159*, 3–30. https://doi.org/10.1016/S0009-2541(99)00031-5

Gong, G.-C., Shiah, F.-K., Liu, K.-K., Wen, Y.-H., & Liang, M.-H. (2000). Spatial and temporal variation of chlorophyll a, primary productivity and chemical hydrography in the southern East China Sea. *Continental Shelf Research*, *20*, 411–436. https://doi.org/10.1016/S0278-4343(99)00079-5

Gong, G.-C., Wen, Y.-H., Wang, B.-W., & Liu, G.-J. (2003). Seasonal variation of chlorophyll a concentration, primary production and environmental conditions in the subtropical East China Sea. *Deep Sea Research Part II: Topical Studies in Oceanography*, *50*, 1219–1236. https://doi.org/10.1016/s0967-0645(03)00019-5

Gruber, N., Hauri, C., Lachkar, Z., Loher, D., Frölicher, T. L., & Plattner, G. K. (2012). Rapid progression of ocean acidification in the California current system. *Science*, *337*(6091), 220–223. https://doi.org/10.1126/science.1216773

Guo, J.-H., Wang, F.-S., Vogt, R. D., Zhang, Y.-H., & Liu, C.-Q. (2015). Anthropogenically enhanced chemical weathering and carbon evasion in the Yangtze Basin. *Scientific Reports*, *5*, 11,941. https://doi.org/10.1038/srep11941

Guo, X.-H., Cai, W.-J., Huang, W.-J., Wang, Y.-C., Chen, F.-Z., Murrell, M. C., et al. (2012). Carbon dynamics and community production in the Mississippi River plume. *Limnology and Oceanorgraphy*, *57*, 1–17. https://doi.org/10.4319/lo.2012.57.1.0001

Guo, X.-H., Cai, W.-J., Zhai, W.-D., Dai, M.-H., Wang, Y.-C., & Chen, B.-S. (2008). Seasonal variations in the inorganic carbon system in the Pearl River (Zhujiang) estuary. *Continental Shelf Research*, *28*, 1424–1434. https://doi.org/10.1016/j.csr.2007.07.011

Guo, X.-H., Zhai, W.-D., Dai, M.-H., Zhang, C., Bai, Y., Xu, Y., et al. (2015). Air-sea $CO_2$ fluxes in the East China Sea based on multiple-year underway observations. *Biogeosciences*, *12*, 5495–5514. https://doi.org/10.5194/bg-12-5495-2015

He, F.-N., Li, M.-J., Li, S.-C., & Xiao, R. (2015). Comparison of changes in land use and land cover in China and the USA over the past 300 years. *Journal of Geographical Sciences*, *25*(9), 1045–1057. https://doi.org/10.1007/s11442-015-1218-3

He, X.-Q., Bai, Y., Pan, D.-L., Chen, C.-T. A., Cheng, Q., Wang, D.-F., & Gong, F. (2013). Satellite views of the seasonal and interannual variability of phytoplankton blooms in the eastern China seas over the past 14 yr (1998–2011). *Biogeosciences*, *10*, 4721–4739. https://doi.org/10.5194/bg-10-4721-2013

Hu, X.-P., Li, Q., Huang, W.-J., Chen, B.-S., Cai, W.-J., Rabalais, N. N., & Turner, R. E. (2017). Effects of eutrophication and benthic respiration on water column carbonate chemistry in a traditional hypoxic zone in the Northern Gulf of Mexico. *Marine Chemistry*, *194*, 33–42. https://doi.org/10.1016/j.marchem.2017.04.004

Huang, W.-J., Wang, Y.-C., & Cai, W.-J. (2012). Assessment of sample storage techniques for total alkalinity and dissolved inorganic carbon in seawater. *Limnology and Oceanography: Methods*, *10*, 711–717. https://doi.org/10.4319/lom.2012.10.711

Huang, X. (2012). The nutrients dynamics and fluxes in the Changjiang Estuary: comparison between the South and North Branches (in Chinese). Master thesis, Xiameng University.

Jiang, L.-Q., Cai, W.-J., Feely, R. A., Wang, Y.-C., Guo, X.-H., Gledhill, D. K., et al. (2010). Carbonate mineral saturation states along the U. S. East Coast. *Limnology and Oceanography*, *55*, 2424–2432. https://doi.org/10.4319/lo.2010.55.6.2424

Joesoef, A., Kirchman, D. L., Sommerfield, C. K., & Cai, W.-J. (2017). Seasonal variability of the inorganic carbon system in a large coastal plain estuary. *Biogeosciences*, *14*, 4949–4963. https://doi.org/10.5194/bg-14-4949-2017

Kaushal, S. S., Likens, G. E., Utz, R. M., Pace, M. L., Grese, M., & Yepsen, M. (2013). Increased river alkalinization in the Eastern U.S. *Environmental Science and Technology*, *47*(18), 10,302–10,311. https://doi.org/10.1021/es401046s

Körtzinger, A. (2003). A significant $CO_2$ sink in the tropical Atlantic Ocean associated with the Amazon River plume. *Geophysical Research Letters*, *30*(24), 2287. https://doi.org/10.1029/2003GL018841

Lefèvre, N., Montes, M. F., Gaspar, F. L., Rocha, C., Jiang, S., De Araújo, M. C., & Ibánhez, J. S. P. (2017). Net heterotrophy in the Amazon continental shelf changes rapidly to a sink of $CO_2$ in the outer Amazon plume. *Frontiers in Marine Science*, *4*, 278. https://doi.org/10.3389/fmars.2017.00278

Lewis, E., & Wallace, D. W. R. (1998). *Program developed for $CO_2$ system calculations, ORNL/CDIAC-105, Carbon Dioxide Information Analysis Center*. Oak Ridge, TN: Oak Ridge National Laboratory, US Department.

Li, C.-L., & Zhai, W.-D. (2019). Decomposing monthly declines in subsurface-water pH and aragonite saturation state from spring to autumn in the North Yellow Sea. *Continental Shelf Research*, *185*, 37–50. https://doi.org/10.1016/j.csr.2018.11.003

Li, J.-Y., & Zhang, J. (2003). Variations of solid content and water chemistry at Nantong station and weathering processes of the Changjiang watershed (in Chinese). *Resources and Environment in the Yangtze Basin*, *12*(4), 363–369.

Liu, P.-F., & Zhai, W.-D. (2016). Optimization of estuarine inorganic carbon water sample storage technique and $pCO_2$ calculation: A case study in the inner Changjiang (Yangtze River) Esurary (in Chinese). *Environmental Chemistry*, *35*(10), 2096–2105.

Liu, X.-C., Shen, H.-T., & Huang, Q.-H. (2002). Concentration variation and flux estimation of dissolved inorganic nutrient from the Changjiang River into its estuary (in Chinese). *Oceanologia et Limnologia Sinica*, *33*(5), 332–340.

Liu, X.-Q., & Wang, S.-M. (2013). Population migration, agricultural development and land utilization patterns in the Yangtze River Basin (in Chinese). *Pratacultural Science*, *30*(12), 2084–2090.

Lukawska-Matuszewska, K. (2016). Contribution of non-carbonate inorganic and organic alkalinity to total measured alkalinity in pore waters in marine sediments (Gulf of Gdansk, S-E Baltic Sea). *Marine Chemistry*, *186*, 211–220. https://doi.org/10.1016/j.marchem.2016.10.002

Mei, X.-F., Dai, Z.-J., Darby, S. E., Gao, S., Wang, J., & Jiang, W.-G. (2018). Modulation of extreme flood levels by impoundment significantly offset by floodplain loss downstream of the Three Gorges Dam. *Geophysical Research Letters*, *45*, 3147–3155. https://doi.org/10.1002/2017GL076935

Meybeck, M. (1993). Riverine transport of atmospheric carbon: sources, global typology and budget. *Water, Air, and Soil Pollution*, *70*, 443–463. https://doi.org/10.1007/978-94-011-1982-5_31

Millero, F. J. (1979). The thermodynamics of the carbonate system in seawater. *Geochimica et Cosmochimica Acta*, *43*, 1651–1661. https://doi.org/10.1016/0016-7037(79)90184-4

Millero, F. J., Graham, T. B., Huang, F., Bustos-Serrano, H., & Pierrot, D. (2006). Dissociation constants of carbonic acid in sea water as a function of salinity and temperature. *Marine Chemistry*, *100*, 80–94. https://doi.org/10.1016/j.marchem.2005.12.001

Mucci, A. (1983). The solubility of calcite and aragonite in seawater at various salinities, temperatures, and one atmosphere total pressure. *American Journal of Science*, *283*, 780–799. https://doi.org/10.2475/ajs.283.7.780

Müller, B., Berg, M., Pernet-Coudrier, B., Qi, W.-X., & Liu, H.-J. (2012). The geochemistry of the Yangtze River: Seasonality of concentrations and temporal trends of chemical loads. *Global Biogeochemical Cycles*, *26*, GB2028. https://doi.org/10.1029/2011GB004273

Ning, X.-R., Shi, J.-X., Cai, Y.-M., & Liu, C.-G. (2004). Biological productivity front in the Changjiang Estuary and the Hangzhou Bay and its ecological effects (in Chinese). *Acta Oceanologica Sinica*, *26*(6), 96–106. http://www.hyxb.org.cn/aos/ch/reader/view_abstract.aspx?file_no=20040611&flag=1

Ning, X.-R., Vaulot, D., Liu, Z.-S., & Liu, Z.-L. (1988). Standing stock and production of phytoplankton in the estuary of the Changjiang (Yangtse River) and the adjacent East China Sea. *Marine Ecology Progress Series*, *49*, 141–150. https://doi.org/10.3354/meps049141

Officer, C. B. (1979). Discussion of the behaviour of nonconservative dissolved constituents in estuaries. *Estuarine and Coastal Marine Science*, *9*(1), 91–94. https://doi.org/10.1016/0302-3524(79)90009-4

Oh, N.-H., & Raymond, P. A. (2006). Contribution of agricultural liming to riverine bicarbonate export and $CO_2$ sequestration in the Ohio River basin. *Global Biogeochemical Cycles*, *20*, GB3012. https://doi.org/10.1029/2005GB002565

Oliveira, A. P., Cabeçadas, G., & Mateus, M. D. (2017). Inorganic carbon distribution and $CO_2$ fluxes in a large European estuary (Tagus, Portugal). *Scientific Reports*, *7*(1), 7376. https://doi.org/10.1038/s41598-017-06758-z

Orr, J. C., Fabry, V. J., Aumont, O., Bopp, L., Doney, S. C., Feely, R. A., et al. (2005). Anthropogenic ocean acidification over the twenty-first century and its impacts on calcifying organisms. *Nature*, *437*(7059), 681–686. https://doi.org/10.1038/nature04095

Pelletier, G. J., Lewis, E., & Wallace, D. W. R. (2015). *CO2SYS.XLS: A calculator for the CO2 system in seawater for Microsoft Excel/VBA, Version 24.* Olympia, Washington: Washington State Department of Ecology.

Peng, T.-H., Hung, J.-J., Wanninkhof, R., & Millero, F.-J. (1999). Carbon budget in the East China Sea in spring. *Tellus Series B: Chemical and Physical Meteorology*, *51*, 531–540. https://doi.org/10.3402/tellusb.v51i2.16337

Prentice, I. C., Farquhar, G. D., Fasham, M. J. R., Goulden, M. L., Heimann, M., Jaramillo, V. J., et al. (2001). The carbon cycle and atmospheric carbon dioxide. In J. T. Houghton, Y. Ding, D. J. Griggs, M. Noguer, P. J. van der Linden, X. Dai, K. Maskell, & C. A. Johnson (Eds.), *Climate Change 2001: The Scientific Basis. Contribution of Working Group I to the Third Assessment Report of the Intergovernmental Panel on Climate Change* (pp. 185–237). Cambridge: Cambridge University Press.

Qi, D. (2013). Dissolved calcium in the Changjiang Estuary and China Seas (in Chinese). Master thesis, Xiameng University.

Ran, X.-B., Liu, S., Liu, J., Zang, J.-Y., Che, H., Ma, Y.-X., & Wang, Y.-B. (2016). Composition and variability in the export of biogenic silica in the Changjiang River and the effect of Three Gorges Reservoir. *Science of the Total Environment*, *571*, 1191–1199. https://doi.org/10.1016/j.scitotenv.2016.07.125

Raymond, P. A., & Cole, J. J. (2003). Increase in the export of alkalinity from North America's largest river. *Science*, *301*(5629), 88–91. https://doi.org/10.1126/science.1083788

Raymond, P. A., Oh, N. H., Turner, R. E., & Broussard, W. (2008). Anthropogenically enhanced fluxes of water and carbon from the Mississippi River. *Nature*, *451*(7177), 449–452. https://doi.org/10.1038/nature06505

Redfield, A. C., Ketchum, B. H., & Richards, F. A. (1963). The influence of organisms on the composition of sea-water. In M. N. Hill (Ed.), *The Sea: ideas and observations on progress in the study of the seas. 2* (pp. 26–77). New York: Interscience Publishers.

Regnier, P., Friedlingstein, P., Ciais, P., Mackenzie, F. T., Gruber, N., Janssens, I. A., et al. (2013). Anthropogenic perturbation of the carbon fluxes from land to ocean. *Nature Geoscience*, *6*, 597–607. https://doi.org/10.1038/ngeo1830

Salisbury, J., Green, M., Hunt, C., & Campbell, J. (2008). Coastal acidification by rivers: a threat to shellfish? *Eos, Transactions American Geophysical Union*, *89*(50), 513–528. https://doi.org/10.1029/2008EO500001

Takahashi, T., Sutherland, S. C., Chipman, D. W., Goddard, J. G., Ho, C., Newberger, T., et al. (2014). Climatological distributions of pH, $pCO_2$, total $CO_2$, alkalinity, and $CaCO_3$ saturation in the global surface ocean, and temporal changes at selected locations. *Marine Chemistry*, *164*, 95–125. https://doi.org/10.1016/j.marchem.2014.06.004

Tan, Y., Zhang, L.-J., Wang, F., & Hu, D.-X. (2004). Summer surface water $pCO_2$ and $CO_2$ flux at air-sea interface in western part of the East China Sea (in Chinese). *Oceanologia et Limnologica Sinica*, *35*, 239–245.

Ternon, J. F., Oudot, C., Dessier, A., & Diverres, D. (2000). A seasonal tropical sink for atmospheric $CO_2$ in the Atlantic Ocean: The role of the Amazon River discharge. *Marine Chemistry*, *68*, 183–201. https://doi.org/10.1016/S0304-4203(99)00077-8

Tseng, C.-M., Shen, P.-Y., & Liu, K.-K. (2014). Synthesis of observed air–sea $CO_2$ exchange fluxes in the river-dominated East China Sea and improved estimates of annual and seasonal net mean fluxes. *Biogeosciences*, *11*, 3855–3870. https://doi.org/10.5194/bg-11-3855-2014

Tsunogai, S., Watanabe, S., & Sato, T. (1999). Is there a "continental shelf pump" for the absorption of atmospheric $CO_2$? *Tellus Series B: Chemical and Physical Meteorology*, *51*, 701–712. https://doi.org/10.3402/tellusb.v51i3.16468

Waldbusser, G. G., Hales, B., Langdon, C. J., Haley, B. A., Schrader, P., Brunner, E. L., et al. (2015). Saturation-state sensitivity of marine bivalve larvae to ocean acidification. *Nature Climate Change*, *5*, 273–280. https://doi.org/10.1038/nclimate2479

Wang, B., Chen, J.-F., Jin, H.-Y., Li, H.-L., Huang, D.-J., & Cai, W.-J. (2017). Diatom bloom-derived bottom water hypoxia off the Changjiang estuary, with and without typhoon influence. *Limnology and Oceanography*, *62*, 1552–1569. https://doi.org/10.1002/lno.10517

Wang, D.-Q., Chen, Z.-L., Xu, S.-Y., Hu, L.-Z., & Wang, J. (2006). Denitrification in Chongming east tidal flat sediment, Yangtze estuary, China. *Science in China Series D: Earth Sciences*, *49*(10), 1090–1097. https://doi.org/10.1007/s11430-006-1090-1

Wang, H.-J., Bi, N.-S., Saito, Y., Wang, Y., Sun, X.-X., Zhang, J., & Yang, Z.-S. (2010). Recent changes in sediment delivery by the Huanghe (Yellow River) to the sea: Causes and environmental implications in its estuary. *Journal of Hydrology*, *391*, 302–313. https://doi.org/10.1016/j.jhydrol.2010.07.030

Wang, H.-J., Yang, Z.-S., Saito, Y., Liu, J. P., & Sun, X.-X. (2006). Interannual and seasonal variation of the Huanghe (Yellow River) water discharge over the past 50 years: Connections to impacts from ENSO events and dams. *Global and Planetary Change*, *50*, 212–225. https://doi.org/10.1016/j.gloplacha.2006.01.005

Wang, J.-H., & Wu, J.-Y. (2009). Occurrence and potential risks of harmful algal blooms in the East China Sea. *Science of the Total Environment*, *407*(13), 4012–4021. https://doi.org/10.1016/j.scitotenv.2009.02.040

Wang, S.-L., Chen, C.-T. A., Hong, G.-H., & Chung, C.-S. (2000). Carbon dioxide and related parameters in the East China Sea. *Continental Shelf Research*, *20*, 525–544. https://doi.org/10.1016/S0278-4343(99)00084-9

Wang, Y.-P., Pan, S.-M., Wang, H. V., Gao, J.-H., Yang, Y., Wang, A.-J., et al. (2006). Measurements and analysis of water discharges and suspended sediment fluxes in Changjiang Estuary (in Chinese). *Acta Geographica Sinica*, *61*(1), 35–46. https://doi.org/10.3321/j.issn:0375-5444.2006.01.004

Wang, Z.-H. A., Bienvenu, D. J., Mann, P. J., Hoering, K. A., Poulsen, J. R., Spencer, R. G. M., & Holmes, R. M. (2013). Inorganic carbon speciation and fluxes in the Congo River. *Geophysical Research Letters*, *40*, 511–516. https://doi.org/10.1002/grl.50160

Wang, Z.-H. A., Wanninkhof, R., Cai, W.-J., Byrne, R. H., Hu, X.-P., Peng, T.-H., & Huang, W.-J. (2013). The marine inorganic carbon system along the Gulf of Mexico and Atlantic coasts of the United States: insights from a transregional coastal carbon study. *Limnology and Oceanography*, *58*, 325–342. https://doi.org/10.4319/lo.2013.58.1.0325

West, T. O., & McBride, A. C. (2005). The contribution of agricultural lime to carbon dioxide emissions in the United States: dissolution, transport, and net emissions. *Agriculture, Ecosystems and Environment*, *108*, 145–154. https://doi.org/10.1016/j.agee.2005.01.002

Wong, G. T. F. (2012). Removal of nitrite interference in the Winkler determination of dissolved oxygen in seawater. *Marine Chemistry*, *130*(131), 28–32. https://doi.org/10.1016/j.marchem.2011.11.003

Wu, Y., Zhang, J., Liu, S.-M., Zhang, Z.-F., Yao, Q.-Z., Hong, G.-H., & Cooper, L. (2007). Sources and distribution of carbon within the Yangtze River system. *Estuarine, Coastal and Shelf Science*, *71*, 13–25. https://doi.org/10.1016/j.ecss.2006.08.016

Zhai, W.-D. (2018). Exploring seasonal acidification in the Yellow Sea. *Science China Earth Sciences*, *61*(6), 647–658. https://doi.org/10.1007/s11430-017-9151-4

Zhai, W.-D., Chen, J.-F., Jin, H.-Y., Li, H.-L., Liu, J.-W., He, X.-Q., & Bai, Y. (2014). Spring carbonate chemistry dynamics of surface waters in the northern East China Sea: water mixing, biological uptake of $CO_2$, and chemical buffering capacity. *Journal of Geophysical Research: Oceans*, *119*, 5638–5653. https://doi.org/10.1002/2014JC009856

Zhai, W.-D., Dai, M.-H., & Guo, X.-H. (2007). Carbonate system and $CO_2$ degassing fluxes in the inner estuary of Changjiang (Yangtze) River, China. *Marine Chemistry*, *107*, 342–356. https://doi.org/10.1016/j.marchem.2007.02.011

Zhai, W.-D., & Hong, H.-S. (2012). $CO_2$ and carbon chemistry in the East China Sea (in Chinese). In H.-S. Hong (Ed.), *Regional Oceanography of China Seas—Chemical Oceanography* (pp. 218–224). Beijing: China Ocean Press.

Zhai, W.-D., Yan, X.-L., & Qi, D. (2017). Biogeochemical generation of dissolved inorganic carbon and nitrogen in the North Branch of inner Changjiang Estuary in a dry season. *Estuarine, Coastal and Shelf Science*, *197*, 136–149. https://doi.org/10.1016/j.ecss.2017.08.027

Zhai, W.-D., Zang, K. P., Huo, C., Zheng, N., & Xu, X. M. (2015). Occurrence of aragonite corrosive water in the North Yellow Sea, near the Yalu River estuary, during a summer flood. *Estuarine, Coastal and Shelf Science*, *166*, 199–208. https://doi.org/10.1016/j.ecss.2015.02.010

Zhai, W.-D., & Zhao, H.-D. (2016). Quantifying air-sea re-equilibration-implied ocean surface $CO_2$ accumulation against recent atmospheric $CO_2$ rise. *Journal of Oceanography*, *72*(4), 651–659. https://doi.org/10.1007/s10872-016-0350-8

Zhai, W.-D., Zheng, N., Huo, C., Xu, Y., Zhao, H.-D., Li, Y.-W., et al. (2014). Subsurface pH and carbonate saturation state of aragonite on the Chinese side of the North Yellow Sea: seasonal variations and controls. *Biogeosciences*, *11*, 1103–1123. https://doi.org/10.5194/bg-11-1103-2014

Zhang, J. (2011). On the critical issues of land-ocean interactions in coastal zones (in Chinese). *Chinese Science Bulletin*, *56*, 1956–1966. https://doi.org/10.1360/972011-465

Zhang, L.-J., Wang, B.-Y., & Zhang, J. (1999). $pCO_2$ in the surface water of the East China Sea in winter and summer (in Chinese). *Journal of Ocean University of Qingdao*, *1999*(Supplement), 149–153.

Zhang, L.-J., Xue, M., Wang, M., Cai, W.-J., Wang, L., & Yu, Z.-G. (2014). The spatiotemporal distribution of dissolved inorganic and organic carbon in the main stem of the Changjiang (Yangtze) River and the effect of the Three Gorges Reservoir. *Journal of Geophysical Research: Biogeosciences*, *119*, 741–757. https://doi.org/10.1002/2012JG002230

Zhang, Y.-H., Huang, Z.-Q., Ma, L.-M., Qiao, R., & Zhang, B. (1997). Carbon dioxide in surface water and its flux in East China Sea (in Chinese). *Journal of Oceanography in Taiwan Strait*, *16*(1), 37–42.

Zhao, Y.-F., Zou, X.-Q., Gao, J.-H., Xu, X., Wang, C.-L., Tang, D.-H., et al. (2015). Quantifying the anthropogenic and climatic contributions to changes in water discharge and sediment load into the sea: A case study of the Yangtze River, China. *Science of the Total Environment*, *536*, 803–812. https://doi.org/10.1016/j.scitotenv.2015.07.119

Zhou, M.-J., Shen, Z.-L., & Yu, R.-C. (2008). Responses of a coastal phytoplankton community to increased nutrient input from the Changjiang (Yangtze) River. *Continental Shelf Research*, *28*, 1483–1489. https://doi.org/10.1016/j.csr.2007.02.009